Journal of the Mechanics and Physics of Solids 97 (2016) 317–332

Contents lists available at ScienceDirect

Journal of the Mechanics and Physics of Solids

journal homepage: www.elsevier.com/locate/jmps

Estimates for the overall linear properties of pointwise heterogeneous solids with application to elasto-viscoplasticity

Martín I. Idiart [b,c], Noel Lahellec [a,*]

[a] Laboratoire de Mécanique et d'Acoustique, CNRS UPR 7051, Aix-Marseille University, Ecole Centrale Marseille, 4 impasse Nikola Tesla, 13453 Marseille Cedex 13, France

[b] Departamento de Aeronáutica, Facultad de Ingeniería, Universidad Nacional de La Plata, Avda. 1 esq. 47 S/N, La Plata B1900TAG, Argentina

[c] Consejo Nacional de Investigaciones Científicas y Técnicas (CONICET), CCT La Plata, Calle 8 No 1467, La Plata B1904CMC, Argentina

ARTICLE INFO

Article history:
Received 2 March 2015
Received in revised form
11 September 2015
Accepted 21 December 2015
Available online 3 March 2016

Keywords:
Heterogeneous materials
Elasto-viscoplasticity
Variational methods
Homogenization

ABSTRACT

New estimates are derived for the overall properties of linear solids with pointwise heterogeneous local properties. The derivation relies on the use of 'comparison solids' which, unlike comparison solids considered previously, are themselves pointwise heterogeneous. The estimates are then exploited within an incremental homogenization scheme to determine the overall response of multiphase elasto-viscoplastic solids under arbitrary loading histories. By way of example, the scheme is applied to incompressible Maxwellian solids with power-law plastic dissipation; particularly simple estimates of the Hashin–Shtrikman type are obtained. Predictions are confronted with full-field simulations for particulate composites under cyclic and rotating loading conditions. Good agreement is found for all cases considered. In particular, elasto-plastic transitions, tension-compression asymmetries (Bauschinger effect) and stress-path distortions induced by material heterogeneity are all well-captured, thus improving significantly on commonly used elastic-plastic decoupled schemes.

1. Scope

Many problems of practical interest in solid mechanics require knowledge of the overall properties of heterogeneous solids in terms of pointwise varying microscopic properties. Prominent examples include the role of residual stresses on the failure processes of engineering alloys and metal composites (e.g., Withers, 2007) and the effect of spontaneous electric polarization on the electromechanical response of ferroelectric composites (e.g., Miehe and Rosato, 2011; Idiart, 2014). Theoretical interest on pointwise heterogeneous solids has also arisen from recent developments initiated by Lahellec and Suquet (2003) on incremental homogenization schemes for predicting the macroscopic response and underlying field statistics in multiphase systems with elasto-viscoplastic behavior. These schemes rely on an implicit time discretization of the elasto-viscoplastic evolution equations together with a suitably designed variational principle governing the state of the solid at the end of the time step, given the state at the beginning of the time step. The latter enters into the scheme as pointwise heterogeneous stress polarizations. Incremental schemes of this sort are intended to improve on classical approaches based on the elasto-plastic tangent approximation (e.g., Hill, 1965) and the affine approximation (e.g., Masson

* Corresponding author.
E-mail addresses: martin.idiart@ing.unlp.edu.ar (M.I. Idiart), lahellec@lma.cnrs-mrs.fr (N. Lahellec).

http://dx.doi.org/10.1016/j.jmps.2015.12.017
0022-5096/

et al., 2000), as well as on decoupled approximations treating the elastic and plastic deformation processes separately (e.g., Aravas and Ponte Castañeda, 2004; Segurado et al., 2012). A recent account on the various schemes so far proposed can be found in Lahellec and Suquet (2013). In any event, central to these incremental schemes is the availability of accurate estimates for the overall properties of pointwise heterogeneous solids with linear local behavior.

It is precisely with a view to developing improved incremental homogenization schemes for elasto-viscoplastic systems that we focus here on linearly viscous solids with a local behavior characterized by

$$\boldsymbol{\sigma}(\mathbf{x}) = \mathbf{L}(\mathbf{x})\dot{\boldsymbol{\varepsilon}}(\mathbf{x}) + \boldsymbol{\tau}(\mathbf{x}), \tag{1}$$

where $\boldsymbol{\sigma}(\mathbf{x})$ and $\dot{\boldsymbol{\varepsilon}}(\mathbf{x})$ denote the Cauchy stress and the infinitesimal strain-rate tensor fields, while $\mathbf{L}(\mathbf{x})$ and $\boldsymbol{\tau}(\mathbf{x})$ denote the local viscosity and pre-stress or stress polarization tensors, respectively, both of which can vary with position $\mathbf{x}$ within the solid. The material response (1) can be written in terms of a quadratic potential function as

$$\boldsymbol{\sigma} = \frac{\partial w}{\partial \dot{\boldsymbol{\varepsilon}}}(\mathbf{x}, \dot{\boldsymbol{\varepsilon}}) \quad \text{where } w(\mathbf{x}, \dot{\boldsymbol{\varepsilon}}) = \frac{1}{2}\dot{\boldsymbol{\varepsilon}}\cdot\mathbf{L}(\mathbf{x})\dot{\boldsymbol{\varepsilon}} + \boldsymbol{\tau}(\mathbf{x})\cdot\dot{\boldsymbol{\varepsilon}}, \tag{2}$$

and, assuming that the viscosity tensor is everywhere positive-definite and that the microstructure exhibits separation of length scales, the overall response of the solid can be written in terms of an effective potential as (see, for instance, Ponte Castañeda and Suquet, 1998)

$$\overline{\boldsymbol{\sigma}} = \frac{\partial \overline{w}}{\partial \overline{\dot{\boldsymbol{\varepsilon}}}}(\overline{\dot{\boldsymbol{\varepsilon}}}) \quad \text{where } \overline{w}(\overline{\dot{\boldsymbol{\varepsilon}}}) = \min_{\dot{\boldsymbol{\varepsilon}} \in \mathcal{K}(\overline{\dot{\boldsymbol{\varepsilon}}})} \langle w(\mathbf{x}, \dot{\boldsymbol{\varepsilon}}) \rangle. \tag{3}$$

In this expression, $\langle\cdot\rangle$ denotes volume averaging over a representative volume element Ω of the heterogeneous solid, $\overline{\boldsymbol{\sigma}} = \langle\boldsymbol{\sigma}\rangle$ and $\overline{\dot{\boldsymbol{\varepsilon}}} = \langle\dot{\boldsymbol{\varepsilon}}\rangle$, and $\mathcal{K}(\overline{\dot{\boldsymbol{\varepsilon}}})$ denotes the set of kinematically admissible strain-rate fields with prescribed volume average $\overline{\dot{\boldsymbol{\varepsilon}}}$.

A general procedure to estimate the effective response (3) in terms of low-order statistics of the local properties (2) has been recently proposed by Lahellec et al. (2011).[1] The procedure relies on the use of 'comparison solids' with *piecewise* heterogeneous properties whose effective potential can be easily estimated or computed exactly. A suitably designed variational statement is used to select the optimal properties that deliver the best possible estimate for the effective potential of the pointwise heterogeneous solid in terms of the effective potential of the piecewise-heterogeneous comparison solid. The resulting estimates have the virtue of improving, necessarily, on elementary estimates based on first-order statistics only, and of delivering bounds under certain conditions. It has been found, however, that the estimates can be quite inaccurate for some classes of pointwise heterogeneous solids which, incidentally, can be relevant to the development of incremental homogenization schemes. It is the case, for instance, of solids with strongly fluctuating polarization fields that are divergence-free. A remedy is proposed in Section 2 by allowing for comparison solids with *pointwise* heterogeneous properties in the variational procedure of Lahellec et al. (2011). This is achieved by making judicious use of divergence-free and compatible fields as comparison polarization stresses. The new linear estimates are then employed in Section 3 within a variant of the incremental homogenization scheme of Lahellec and Suquet (2013) to estimate the overall response of elasto-viscoplastic multiphase systems made up of Maxwellian phases. In the case of incompressible solids with power-law plastic dissipation, particularly simple estimates of the Hashin–Shtrikman type are obtained. Sample results for complex loading histories are confronted with decoupled estimates and full-field simulations in Section 4. Finally, some concluding remarks are given in Section 4.2.

2. Estimates based on pointwise heterogeneous comparison solids

2.1. Variational framework

We begin by introducing a 'comparison solid' with local potential

$$w_0(\mathbf{x}, \dot{\boldsymbol{\varepsilon}}) = \frac{1}{2}\dot{\boldsymbol{\varepsilon}}\cdot\mathbf{L}_0(\mathbf{x})\dot{\boldsymbol{\varepsilon}} + \boldsymbol{\tau}_0(\mathbf{x})\cdot\dot{\boldsymbol{\varepsilon}}, \tag{4}$$

where $\mathbf{L}_0(\mathbf{x})$ and $\boldsymbol{\tau}_0(\mathbf{x})$ are local properties within a certain class C to be specified. Then, upon defining the function

$$V(\mathbf{L}_0, \boldsymbol{\tau}_0) = \sup_{\dot{\boldsymbol{\varepsilon}}(\mathbf{x})} \left\langle w(\mathbf{x}, \dot{\boldsymbol{\varepsilon}}) - w_0(\mathbf{x}, \dot{\boldsymbol{\varepsilon}}) \right\rangle, \tag{5}$$

we have the inequality

$$\langle w(\mathbf{x}, \dot{\boldsymbol{\varepsilon}}) \rangle \le \langle w_0(\mathbf{x}, \dot{\boldsymbol{\varepsilon}}) \rangle + V(\mathbf{L}_0, \boldsymbol{\tau}_0) \tag{6}$$

for any set of admissible comparison properties and strain-rate field. In view of (3), this inequality generates the upper

[1] The procedure was proposed in the mathematically analogous context of thermoelasticity.

bound on the effective potential

$$\widetilde{W}(\bar{\boldsymbol{\varepsilon}}) \le \widetilde{W}_+(\bar{\boldsymbol{\varepsilon}}) = \inf_{\mathbf{L}_0,\boldsymbol{\tau}_0\in C}[\widetilde{W}_0(\bar{\boldsymbol{\varepsilon}};\mathbf{L}_0,\boldsymbol{\tau}_0) + V(\mathbf{L}_0,\boldsymbol{\tau}_0)], \tag{7}$$

where $\widetilde{W}_0$ is the effective potential of the comparison solid as given by

$$\widetilde{W}_0(\bar{\boldsymbol{\varepsilon}};\mathbf{L}_0,\boldsymbol{\tau}_0) = \min_{\dot{\boldsymbol{\varepsilon}}\in\mathcal{K}(\bar{\boldsymbol{\varepsilon}})}\langle w_0(\mathbf{x},\dot{\boldsymbol{\varepsilon}})\rangle = \frac{1}{2}\bar{\boldsymbol{\varepsilon}}\cdot\widetilde{\mathbf{L}}_0\bar{\boldsymbol{\varepsilon}} + \widetilde{\boldsymbol{\tau}}_0\cdot\bar{\boldsymbol{\varepsilon}} + \widetilde{f}_0. \tag{8}$$

In this expression, $\widetilde{\mathbf{L}}_0$, $\widetilde{\boldsymbol{\tau}}_0$ and $\widetilde{f}_0$ are the effective properties of the comparison solid.

The optimization with respect to the comparison properties in (7) yields the best possible bound that can be obtained with the class of comparison solids admitted. The larger the class, the potentially sharper the bound. Furthermore, if the class of comparison solids admitted includes the pointwise heterogeneous solid, the bound (7) reduces to the exact result. In any case, the optimal viscosity will be such that $\mathbf{L}_0 \ge \mathbf{L}$, given that the function V is infinite otherwise. Given this inequality, the supremum operation in the function V can be performed explicitly by differentiation giving

$$V(\mathbf{L}_0,\boldsymbol{\tau}_0) = -\frac{1}{2}\left\langle \Delta\boldsymbol{\tau}(\mathbf{x})\cdot(\Delta\mathbf{L}(\mathbf{x}))^{-1}\Delta\boldsymbol{\tau}(\mathbf{x})\right\rangle, \tag{9}$$

where $\Delta\mathbf{L}(\mathbf{x}) = \mathbf{L}(\mathbf{x}) - \mathbf{L}_0(\mathbf{x})$ and $\Delta\boldsymbol{\tau}(\mathbf{x}) = \boldsymbol{\tau}(\mathbf{x}) - \boldsymbol{\tau}_0(\mathbf{x})$. Finally, an estimate for the overall stress–strain-rate relation can be obtained by differentiating (7). In view of the optimality of (7) with respect to the comparison properties, it can be shown that

$$\bar{\boldsymbol{\sigma}} = \frac{\partial\widetilde{W}_+}{\partial\bar{\boldsymbol{\varepsilon}}}(\bar{\boldsymbol{\varepsilon}}) = \frac{\partial\widetilde{W}_0}{\partial\bar{\boldsymbol{\varepsilon}}}(\bar{\boldsymbol{\varepsilon}};\mathbf{L}_0,\boldsymbol{\tau}_0) = \widetilde{\mathbf{L}}_0\bar{\boldsymbol{\varepsilon}} + \widetilde{\boldsymbol{\tau}}_0, \tag{10}$$

where $\widetilde{\mathbf{L}}_0$ and $\widetilde{\boldsymbol{\tau}}_0$ are evaluated at the optimal values of $\mathbf{L}_0$ and $\boldsymbol{\tau}_0$.

2.2. Estimates based on pointwise-heterogeneous comparison solids

The estimate (7) is useful provided the class of comparison solids (4) allows the effective potential (8) to be computed. In view of this proviso, we consider comparison solids with local properties of the form:

$$\mathbf{L}_0(\mathbf{x}) = \sum_{r=1}^{N}\chi_0^{(r)}(\mathbf{x})\mathbf{L}_0^{(r)} \quad\text{and}\quad \boldsymbol{\tau}_0(\mathbf{x}) = \sum_{r=1}^{N}\chi_0^{(r)}(\mathbf{x})\boldsymbol{\tau}_0^{(r)} + \alpha_0\mathbf{s}_0(\mathbf{x}) + \beta_0\mathbf{L}_0(\mathbf{x})\boldsymbol{\gamma}_0(\mathbf{x}), \tag{11}$$

where $\chi_0^{(r)}(\mathbf{x})$ are prescribed characteristic functions of N – possibly disconnected – subdomains $\Omega_0^{(r)} \subset \Omega$, such that $\cup_{r=1}^{N}\Omega_0^{(r)} = \Omega$, while $\mathbf{s}_0(\mathbf{x})$ and $\boldsymbol{\gamma}_0(\mathbf{x})$ are prescribed tensor fields satisfying the differential constraints:

$$\nabla\cdot\mathbf{s}_0(\mathbf{x}) = \mathbf{0} \quad\text{in } \Omega \quad\text{and}\quad \langle\mathbf{s}_0\rangle = \mathbf{0}, \tag{12}$$

$$\boldsymbol{\gamma}_0(\mathbf{x}) = \nabla\otimes_s\ \mathbf{v}_0(\mathbf{x}) \quad\text{in } \Omega \quad\text{and}\quad \langle\boldsymbol{\gamma}_0\rangle = \mathbf{0}, \tag{13}$$

where ∇ denotes the standard nabla operator and $\otimes_s$ refers to the symmetric part of the tensor product. That is, the field $\mathbf{s}_0$ is divergence-free while the field $\boldsymbol{\gamma}_0$ is compatible.

Thus, comparison solids within the class (11) have *piecewise* heterogeneous viscosity but *pointwise* heterogeneous stress polarization. Now, it is shown in Appendix A that, in view of conditions (12)–(13), the effective potential (8) for this class of comparison solids is given by

$$\widetilde{W}_0(\bar{\boldsymbol{\varepsilon}};\mathbf{L}_0,\boldsymbol{\tau}_0) = \hat{W}_0(\bar{\boldsymbol{\varepsilon}};\mathbf{L}_0^{(s)},\boldsymbol{\tau}_0^{(s)}) + \hat{V}_0(\mathbf{L}_0^{(s)},\boldsymbol{\tau}_0^{(s)},\beta_0), \tag{14}$$

where

$$\hat{W}_0(\bar{\boldsymbol{\varepsilon}};\mathbf{L}_0^{(s)},\boldsymbol{\tau}_0^{(s)}) = \min_{\dot{\boldsymbol{\varepsilon}}\in\mathcal{K}(\bar{\boldsymbol{\varepsilon}})}\sum_{r=1}^{N}c_0^{(r)}\left\langle\frac{1}{2}\dot{\boldsymbol{\varepsilon}}\cdot\mathbf{L}_0^{(r)}\dot{\boldsymbol{\varepsilon}} + \boldsymbol{\tau}_0^{(r)}\cdot\dot{\boldsymbol{\varepsilon}}\right\rangle^{(r)} = \frac{1}{2}\bar{\boldsymbol{\varepsilon}}\cdot\widetilde{\mathbf{L}}_0\bar{\boldsymbol{\varepsilon}} + \widetilde{\boldsymbol{\tau}}_0\cdot\bar{\boldsymbol{\varepsilon}} + \hat{f}_0 \tag{15}$$

and

$$\hat{V}_0(\mathbf{L}_0^{(s)},\boldsymbol{\tau}_0^{(s)},\beta_0) = \sum_{r=1}^{N}c_0^{(r)}\left\langle\frac{1}{2}\beta_0^2\boldsymbol{\gamma}_0\cdot\mathbf{L}_0^{(r)}\boldsymbol{\gamma}_0 - \beta_0\boldsymbol{\tau}_0^{(r)}\cdot\boldsymbol{\gamma}_0\right\rangle^{(r)}. \tag{16}$$

In these expressions, $\langle\cdot\rangle^{(r)}$ denotes volume average over $\Omega_0^{(r)}$ with volume fraction $c_0^{(r)}$. Note that the potentials $\widetilde{w}_0$ and $\hat{w}_0$ are quadratic functions of $\bar{\boldsymbol{\varepsilon}}$ with the same $\widetilde{\mathbf{L}}_0$ and $\widetilde{\boldsymbol{\tau}}_0$ but with different constant terms related by $\widetilde{f}_0 = \hat{f}_0 + \hat{v}_0$. These effective properties can be expressed as (Willis, 1981)

$$\widetilde{\mathbf{L}}_0 = \sum_{r=1}^{N} c_0^{(r)} \mathbf{L}_0^{(r)} \mathbf{A}^{(r)}, \quad \widetilde{\boldsymbol{\tau}}_0 = \sum_{r=1}^{N} c_0^{(r)} (\mathbf{A}^{(r)})^T \boldsymbol{\tau}_0^{(r)}, \quad \hat{f}_0 = \frac{1}{2} \sum_{r=1}^{N} c_0^{(r)} \mathbf{a}^{(r)} \cdot \boldsymbol{\tau}_0^{(r)}, \tag{17}$$

where $\mathbf{A}^{(r)}$ and $\mathbf{a}^{(r)}$ are strain-rate concentration tensors, which depend on all tensors $\mathbf{L}_0^{(s)}$ and $\boldsymbol{\tau}_0^{(s)}$, such that $\langle \dot{\boldsymbol{\varepsilon}}_c \rangle^{(r)} = \mathbf{A}^{(r)} \bar{\dot{\boldsymbol{\varepsilon}}} + \mathbf{a}^{(r)}$, with $\dot{\boldsymbol{\varepsilon}}_c$ being the minimizing strain-rate field in the comparison problem (15).

Introducing expression (14) in (7) we obtain the bound

$$\widetilde{W}_+(\bar{\dot{\boldsymbol{\varepsilon}}}) = \inf_{\substack{\mathbf{L}_0^{(r)}, \boldsymbol{\tau}_0^{(r)} \\ \alpha_0, \beta_0}} \left[\hat{W}_0\left(\bar{\dot{\boldsymbol{\varepsilon}}}; \mathbf{L}_0^{(s)}, \boldsymbol{\tau}_0^{(s)}\right) + \hat{V}_0\left(\mathbf{L}_0^{(s)}, \boldsymbol{\tau}_0^{(s)}, \beta_0\right) + V\left(\mathbf{L}_0^{(s)}, \boldsymbol{\tau}_0^{(s)}, \alpha_0, \beta_0\right) \right], \tag{18}$$

where $\hat{W}_0$, as given by (15), is the effective potential of a *piecewise* heterogeneous solid with N phases characterized by $\Omega_0^{(r)}$, $\mathbf{L}_0^{(r)}$ and $\boldsymbol{\tau}_0^{(r)}$, and the function V is given by

$$V(\mathbf{L}_0^{(s)}, \boldsymbol{\tau}_0^{(s)}, \alpha_0, \beta_0) = -\frac{1}{2} \sum_{r=1}^{N} c_0^{(r)} \left\langle \left(\boldsymbol{\tau} - \boldsymbol{\tau}_0^{(r)} - \alpha_0 \mathbf{s}_0 - \beta_0 \mathbf{L}_0^{(r)} \boldsymbol{\gamma}_0\right) \cdot \left(\mathbf{L} - \mathbf{L}_0^{(r)}\right)^{-1} \left(\boldsymbol{\tau} - \boldsymbol{\tau}_0^{(r)} - \alpha_0 \mathbf{s}_0 - \beta_0 \mathbf{L}_0^{(r)} \boldsymbol{\gamma}_0\right) \right\rangle^{(r)} \tag{19}$$

with a slight abuse of notation. Thus, expression (18) allows the use of available upper bounds or exact results for piecewise heterogeneous solids to generate bounds for pointwise heterogeneous solids. The bound contains information about the properties of the pointwise heterogeneous solid in the form of the first and second moments within each phase domain $\Omega_0^{(r)}$ and of pondered first moments within the entire domain $\boldsymbol{\Omega}$, of certain combination of $\mathbf{L}(\mathbf{x})$ and $\boldsymbol{\tau}(\mathbf{x})$. To see this, note that the objective function in (18) is convex in the comparison properties so that any stationary point satisfying the inequality $\mathbf{L}_0 \geq \mathbf{L}$ is an extremal point. The stationarity conditions are given by

$$-\langle \dot{\boldsymbol{\varepsilon}}_c \rangle^{(r)} = \langle \Delta \mathbf{L}^{-1} \Delta \boldsymbol{\tau} \rangle^{(r)} - \beta_0 \langle \boldsymbol{\gamma}_0 \rangle^{(r)}, \tag{20}$$

$$\langle \dot{\boldsymbol{\varepsilon}}_c \otimes \dot{\boldsymbol{\varepsilon}}_c \rangle^{(r)} = \langle \Delta \mathbf{L}^{-1} \Delta \boldsymbol{\tau} \otimes \Delta \mathbf{L}^{-1} \Delta \boldsymbol{\tau} \rangle^{(r)} - 2\beta_0 \left\langle \boldsymbol{\gamma}_0 \otimes_s \Delta \mathbf{L}^{-1} \Delta \boldsymbol{\tau} \right\rangle^{(r)} - \beta_0^2 \langle \boldsymbol{\gamma}_0 \otimes \boldsymbol{\gamma}_0 \rangle^{(r)}, \tag{21}$$

$$0 = \langle \mathbf{s}_0 \cdot \Delta \mathbf{L}^{-1} \Delta \boldsymbol{\tau} \rangle, \tag{22}$$

$$0 = \left\langle \mathbf{L}_0 \boldsymbol{\gamma}_0 \cdot \Delta \mathbf{L}^{-1} \Delta \boldsymbol{\tau} \right\rangle + \beta_0 \langle \boldsymbol{\gamma}_0 \cdot \mathbf{L}_0 \boldsymbol{\gamma}_0 \rangle - \sum_{r=1}^{N} c_0^{(r)} \boldsymbol{\tau}_0^{(r)} \cdot \langle \boldsymbol{\gamma}_0 \rangle^{(r)}, \tag{23}$$

where $\dot{\boldsymbol{\varepsilon}}_c$ is the strain-rate field in the optimal comparison solid; in deriving these conditions, use has been made of the stationarity condition in the function V and of the well-known identities (e.g., Ponte Castañeda and Suquet, 1998)

$$\langle \dot{\boldsymbol{\varepsilon}}_c \rangle^{(r)} = \frac{1}{c_0^{(r)}} \frac{\partial \widetilde{W}_0}{\partial \boldsymbol{\tau}_0^{(r)}} \quad \text{and} \quad \langle \dot{\boldsymbol{\varepsilon}}_c \otimes \dot{\boldsymbol{\varepsilon}}_c \rangle^{(r)} = \frac{2}{c_0^{(r)}} \frac{\partial \widetilde{W}_0}{\partial \mathbf{L}_0^{(r)}}. \tag{24}$$

Expressions (20) through (23) constitute a coupled system of non-linear algebraic equations for the comparison properties $\mathbf{L}_0^{(r)}$, $\boldsymbol{\tau}_0^{(r)}$, α_0 and β_0 which must be solved numerically, in general. Once the solution is determined, the overall response of the pointwise heterogeneous solid can be estimated via (10) with $\widetilde{\mathbf{L}}_0$ and $\widetilde{\boldsymbol{\tau}}_0$ being the effective properties of the optimal piecewise heterogeneous solid (15).

A few facts regarding the bound (7) are worth noting. Firstly, it is noted that the fields $\mathbf{s}_0(\mathbf{x})$ and $\boldsymbol{\gamma}_0(\mathbf{x})$ have been taken here as prescribed. Potentially sharper bounds would certainly result from optimizing with respect to these fields, but the optimality conditions will not be algebraic in view of the differential constraints imposed by the divergence-free and compatibility conditions. Sharper bounds would also result from optimizing with respect to the characteristic functions $\chi_0^{(r)}(\mathbf{x})$, that is, with respect to the microstructure of the comparison solid, but this is also likely to lead to complicated optimality conditions. In practice, heterogeneous solids usually have a certain microstructural morphology with distinct domains which can be taken as the microstructure of the comparison solid. Secondly, if the effective potential $\hat{W}_0$ of the piecewise heterogeneous solid is estimated approximately rather than computed exactly or bounded from above, expression (7) ceases to be an upper bound but expression (10) still delivers an estimate for the overall stress–strain-rate response. Thirdly, a corresponding lower bound can be derived by replacing the supremum by an infimum operation in the definition of the function V, as given by (5), and following a completely analogous derivation. Fourthly, we note that a weaker but considerably simpler bound results from use of the subclass of comparison solids with $\beta_0 = 0$. In this case, the bound reduces to

$$\widetilde{W}'_+(\bar{\dot{\boldsymbol{\varepsilon}}}) = \inf_{\mathbf{L}_0^{(r)}, \boldsymbol{\tau}_0^{(r)}, \alpha_0} \left[\hat{W}_0\left(\bar{\dot{\boldsymbol{\varepsilon}}}; \mathbf{L}_0^{(s)}, \boldsymbol{\tau}_0^{(s)}\right) + V\left(\mathbf{L}_0^{(s)}, \boldsymbol{\tau}_0^{(s)}, \alpha_0, 0\right) \right], \tag{25}$$

and the associated optimality conditions reduce to

$$-\langle \dot{\boldsymbol{\varepsilon}}_c \rangle^{(r)} = \langle \Delta \mathbf{L}^{-1} \Delta \boldsymbol{\tau} \rangle^{(r)} \quad \text{and} \quad \langle \dot{\boldsymbol{\varepsilon}}_c \otimes \dot{\boldsymbol{\varepsilon}}_c \rangle^{(r)} = \langle \Delta \mathbf{L}^{-1} \Delta \boldsymbol{\tau} \otimes \Delta \mathbf{L}^{-1} \Delta \boldsymbol{\tau} \rangle^{(r)}, \tag{26}$$

together with (22). These conditions imply that

$$\mathbf{C}^{(r)}(\dot{\boldsymbol{\varepsilon}}_c) = \mathbf{C}^{(r)}(\Delta \mathbf{L}^{-1} \Delta \boldsymbol{\tau}), \tag{27}$$

where $\mathbf{C}^{(r)}(\mathbf{a}) \doteq \langle (\mathbf{a} - \langle \mathbf{a} \rangle^{(r)}) \otimes (\mathbf{a} - \langle \mathbf{a} \rangle^{(r)}) \rangle^{(r)}$ denotes the fluctuation tensor of a field $\mathbf{a}(\mathbf{x})$ within phase r. Bounds based on piecewise-heterogeneous comparison solids can be obtained by further restricting the above class of comparison solids to those with $\alpha_0 = \beta_0 = 0$ in (11):

$$\widetilde{W}_+''(\bar{\boldsymbol{\varepsilon}}) = \inf_{\mathbf{L}_0^{(r)}, \boldsymbol{\tau}_0^{(r)}} \left[\hat{w}_0\left(\bar{\boldsymbol{\varepsilon}}; \mathbf{L}_0^{(s)}, \boldsymbol{\tau}_0^{(s)}\right) + V\left(\mathbf{L}_0^{(s)}, \boldsymbol{\tau}_0^{(s)}, 0, 0\right) \right] \tag{28}$$

with optimality conditions given by (26). This is the bound originally proposed by Lahellec et al. (2011), which, in general, should be weaker than the bounds (18) and (25).

The improvement of the new bounds (18) and (25) over the earlier bound (28) can be particularly notorious when the stress polarization field $\boldsymbol{\tau}(\mathbf{x})$ is divergence-free and strongly heterogeneous. In this case, Hill's lemma implies that the exact overall response (3) depends solely on the average value $\langle \boldsymbol{\tau}(\mathbf{x}) \rangle$. It is easy to see that by identifying $\mathbf{s}_0(\mathbf{x})$ with $\boldsymbol{\tau}(\mathbf{x}) - \langle \boldsymbol{\tau}(\mathbf{x}) \rangle$, the bounds (18) and (25) for this class of solids also depend on the stress polarization field through its average value only. By contrast, the bound (28) will, in general, depend on phase averages and intraphase fluctuations of the stress polarization field through conditions (26) and (27), and can therefore differ significantly from the sharper bounds (18) and (25) when the polarization stress field exhibits strong spatial fluctuations.

3. Application to elasto-viscoplastic multiphase solids

The estimates derived in the previous section are exploited here in the context of an incremental homogenization scheme to estimate the overall response of elasto-viscoplastic multiphase solids. We assume the solids are made up of N homogeneous phases occupying domains $\Omega^{(r)} \subset \Omega$ $(r = 1, \ldots, N)$ with characteristic functions $\chi^{(r)}(\mathbf{x})$, and exhibiting separation of length scales.

3.1. Local response of constituent phases

The elasto-viscoplastic response of the local constituents is described within the framework of generalized standard materials by constitutive relations of the form (Germain et al., 1983)

$$\boldsymbol{\sigma} = \frac{\partial w}{\partial \boldsymbol{\varepsilon}}(\mathbf{x}, \boldsymbol{\varepsilon}, \boldsymbol{\alpha}) \quad \text{and} \quad \frac{\partial w}{\partial \boldsymbol{\alpha}}(\mathbf{x}, \boldsymbol{\varepsilon}, \boldsymbol{\alpha}) + \frac{\partial \varphi}{\partial \dot{\boldsymbol{\alpha}}}(\mathbf{x}, \dot{\boldsymbol{\alpha}}) = \mathbf{0}, \tag{29}$$

where

$$w(\mathbf{x}, \boldsymbol{\varepsilon}, \boldsymbol{\alpha}) = \sum_{r=1}^{N} \chi^{(r)}(\mathbf{x}) w^{(r)}(\boldsymbol{\varepsilon}, \boldsymbol{\alpha}) \quad \text{and} \quad \varphi(\mathbf{x}, \dot{\boldsymbol{\alpha}}) = \sum_{r=1}^{N} \chi^{(r)}(\mathbf{x}) \varphi^{(r)}(\dot{\boldsymbol{\alpha}}). \tag{30}$$

In these expressions, $\boldsymbol{\alpha}$ is a tensorial internal variable representing the plastic strain, and the functions $w^{(r)}$ and $\varphi^{(r)}$ denote, respectively, the free-energy density and the dissipation potential of phase r. Even though the homogenization scheme considered below admits quite general constitutive relations, to ease the presentation we restrict attention to isotropic phases characterized by

$$w^{(r)}(\boldsymbol{\varepsilon}, \boldsymbol{\alpha}) = \frac{1}{2}(\boldsymbol{\varepsilon} - \boldsymbol{\alpha}) \cdot \boldsymbol{\mathcal{L}}^{(r)} (\boldsymbol{\varepsilon} - \boldsymbol{\alpha}) \quad \text{and} \quad \varphi^{(r)}(\dot{\boldsymbol{\alpha}}) = \begin{cases} \phi^{(r)}(\dot{\alpha}_{eq}) & \text{if } \operatorname{tr} \dot{\boldsymbol{\alpha}} = 0 \\ +\infty & \text{otherwise} \end{cases} \tag{31}$$

with $\boldsymbol{\mathcal{L}}^{(r)} = 3\kappa^{(r)} \mathbf{J} + 2\mu^{(r)} \mathbf{K}$, where $\kappa^{(r)}$ and $\mu^{(r)}$ denote, respectively, the bulk and shear elastic moduli of the solid, $\mathbf{J}$ and $\mathbf{K}$ are fourth-order tensors corresponding to the standard hydrostatic and shear isotropic projections, and $\phi^{(r)}$ is a positive, convex function of the equivalent plastic strain rate $\dot{\alpha}_{eq} = \sqrt{(2/3)\dot{\boldsymbol{\alpha}} \cdot \dot{\boldsymbol{\alpha}}}$, such that $\phi^{(r)}(0) = 0$. Note that, in view of (29), the potentials (31) correspond to the Maxwellian constitutive relation

$$\dot{\boldsymbol{\varepsilon}} = (\boldsymbol{\mathcal{L}}^{(r)})^{-1} \dot{\boldsymbol{\sigma}} + \frac{\partial \varphi^{(r)\star}}{\partial \boldsymbol{\sigma}}(\boldsymbol{\sigma}), \tag{32}$$

where $\varphi^{(r)\star}$ is the Legendre dual of $\varphi^{(r)}$.

3.2. Overall response of multiphase solid and field statistics

We now make use of the variational representation of Lahellec and Suquet (2013) for the overall response of multiphase

solids with local behavior (29). In this representation, the field equations are discretized in time ($t_0 = 0$, t_1, …, t_n, t_{n+1}, …, $t_N = T$) and the constitutive relations (29) are expressed as

$$\boldsymbol{\sigma}_{n+1} = \frac{\partial w_\Delta}{\partial \dot{\boldsymbol{\varepsilon}}}(\mathbf{x}, \dot{\boldsymbol{\varepsilon}}; \boldsymbol{\varepsilon}_n, \boldsymbol{\alpha}_n), \tag{33}$$

where $\boldsymbol{\sigma}_{n+1}$ is the stress at time t_{n+1}, $\boldsymbol{\varepsilon}_n$ and $\boldsymbol{\alpha}_n$ are the strain and plastic strain at time t_n, $\dot{\boldsymbol{\varepsilon}}$ is the strain rate during the time interval (t_n, t_{n+1}), and

$$w_\Delta(\mathbf{x}, \dot{\boldsymbol{\varepsilon}}; \boldsymbol{\varepsilon}_n, \boldsymbol{\alpha}_n) = \min_{\dot{\boldsymbol{\alpha}}} \left\{ \frac{1}{\Delta t}[w(\mathbf{x}, \boldsymbol{\varepsilon}_n + \Delta t\dot{\boldsymbol{\varepsilon}}, \boldsymbol{\alpha}_n + \Delta t\dot{\boldsymbol{\alpha}}) - w(\mathbf{x}, \boldsymbol{\varepsilon}_n, \boldsymbol{\alpha}_n)] + \varphi(\mathbf{x}, \dot{\boldsymbol{\alpha}}) \right\} \tag{34}$$

is an incremental rate potential for the time step $\Delta t = t_{n+1} - t_n$. The minimization condition with respect to the plastic strain rate in this expression implies the discretized evolution law $(29)_2$.

The constitutive relation (33) is akin to that of a non-linearly viscous solid. Therefore, the relation between the macroscopic stress at time t_{n+1} and the macroscopic strain rate during the interval (t_n, t_{n+1}) can be expressed as

$$\overline{\boldsymbol{\sigma}}_{n+1} = \frac{\partial \widetilde{W}_\Delta}{\partial \dot{\overline{\boldsymbol{\varepsilon}}}}(\dot{\overline{\boldsymbol{\varepsilon}}}; \boldsymbol{\varepsilon}_n, \boldsymbol{\alpha}_n), \tag{35}$$

where

$$\widetilde{W}_\Delta(\dot{\overline{\boldsymbol{\varepsilon}}}; \boldsymbol{\varepsilon}_n, \boldsymbol{\alpha}_n) = \min_{\dot{\boldsymbol{\varepsilon}} \in \mathcal{K}(\dot{\overline{\boldsymbol{\varepsilon}}})} \langle w_\Delta(\mathbf{x}, \dot{\boldsymbol{\varepsilon}}; \boldsymbol{\varepsilon}_n, \boldsymbol{\alpha}_n) \rangle \tag{36}$$

is an incremental effective potential. This variational representation based on strain rates is a convenient alternative to the representation of Miehe (2002) and Lahellec and Suquet (2003, 2007a,b) based on strains. In any case, note that the effective incremental potential depends on the strain and plastic strain fields within the solid from the previous time step. Our purpose is to derive approximate estimates that depend on low-order statistics of these fields rather than on the entire fields, thus providing a description of the overall response in terms of a *finite* number of macroscopic internal variables.

In the case of constituent phases characterized by (31), the incremental effective potential (36) is given by

$$\widetilde{W}_\Delta(\dot{\overline{\boldsymbol{\varepsilon}}}; \boldsymbol{\sigma}_n) = \min_{\dot{\boldsymbol{\varepsilon}} \in \mathcal{K}(\dot{\overline{\boldsymbol{\varepsilon}}})} \min_{\dot{\boldsymbol{\alpha}} \in \mathcal{A}} \left\langle \frac{\Delta t}{2}(\dot{\boldsymbol{\varepsilon}} - \dot{\boldsymbol{\alpha}}) \cdot \boldsymbol{\mathcal{L}}(\mathbf{x})(\dot{\boldsymbol{\varepsilon}} - \dot{\boldsymbol{\alpha}}) + \boldsymbol{\sigma}_n(\mathbf{x}) \cdot (\dot{\boldsymbol{\varepsilon}} - \dot{\boldsymbol{\alpha}}) + \phi(\mathbf{x}, \dot{\alpha}_{eq}) \right\rangle, \tag{37}$$

where $\mathcal{A}$ denotes the set of traceless plastic strain-rate fields, $\boldsymbol{\sigma}_n(\mathbf{x}) = \boldsymbol{\mathcal{L}}(\mathbf{x})(\boldsymbol{\varepsilon}_n(\mathbf{x}) - \boldsymbol{\alpha}_n(\mathbf{x}))$ is the stress field within the solid from the previous time step, and $\boldsymbol{\mathcal{L}}(\mathbf{x}) = \sum_{r=1}^{N} \chi^{(r)}(\mathbf{x}) \boldsymbol{\mathcal{L}}^{(r)}$. The estimates derived in section 3.4.1 below will depend on the first and second moments of the deviatoric stress field $\boldsymbol{\sigma}_n^d(\mathbf{x})$ within each phase r. Their time integration thus requires the computation of these statistics at time step t_{n+1}. To that end, use can be made of the identities

$$\langle \boldsymbol{\sigma}_{n+1}^d \rangle^{(r)} = \langle \boldsymbol{\sigma}_n^d \rangle^{(r)} + 2\mu^{(r)} \Delta t \frac{1}{c^{(r)}} \frac{\partial \widetilde{W}_{\Delta p}}{\partial \mathbf{p}^{(r)}}\bigg|_{\mathbf{p}^{(s)} = \mathbf{0}} \tag{38}$$

and

$$\langle \boldsymbol{\sigma}_{n+1}^d \cdot \boldsymbol{\sigma}_{n+1}^d \rangle^{(r)} = \langle \boldsymbol{\sigma}_n^d \cdot \boldsymbol{\sigma}_n^d \rangle^{(r)} + \frac{(2\mu^{(r)})^2 \Delta t}{c^{(r)}} \frac{\partial \widetilde{W}_\Delta}{\partial \mu^{(r)}} + \frac{4\mu^{(r)} \Delta t}{c^{(r)}} \frac{\partial \widetilde{W}_{\Delta p}}{\partial p^{(r)}}\bigg|_{p^{(s)} = 1}, \tag{39}$$

where

$$\widetilde{W}_{\Delta p}(\dot{\overline{\boldsymbol{\varepsilon}}}; \boldsymbol{\sigma}_n, \mathbf{p}^{(s)}, p^{(s)}) = \min_{\dot{\boldsymbol{\varepsilon}} \in \mathcal{K}(\dot{\overline{\boldsymbol{\varepsilon}}})} \min_{\dot{\boldsymbol{\alpha}} \in \mathcal{A}} \left\langle \frac{\Delta t}{2}(\dot{\boldsymbol{\varepsilon}} - \dot{\boldsymbol{\alpha}}) \cdot \boldsymbol{\mathcal{L}}(\mathbf{x})(\dot{\boldsymbol{\varepsilon}} - \dot{\boldsymbol{\alpha}}) + [\boldsymbol{\sigma}_n^s(\mathbf{x}) + p(\mathbf{x})\boldsymbol{\sigma}_n^d(\mathbf{x}) + \mathbf{p}(\mathbf{x})] \cdot (\dot{\boldsymbol{\varepsilon}} - \dot{\boldsymbol{\alpha}}) + \phi(\mathbf{x}, \dot{\alpha}_{eq}) \right\rangle \tag{40}$$

is a perturbed effective potential with perturbation parameters $\mathbf{p}(\mathbf{x}) = \sum_{r=1}^{N} \chi^{(r)}(\mathbf{x}) \mathbf{p}^{(r)}$ and $p(\mathbf{x}) = \sum_{r=1}^{N} \chi^{(r)}(\mathbf{x}) p^{(r)}$ such that $tr\,(\mathbf{p}^{(r)}) = 0$, and $\boldsymbol{\sigma}_n^s(\mathbf{x})$ denotes the spherical stress field from the previous time step. These identities follow from arguments given in Idiart and Ponte Castañeda (2007).

3.3. Estimates based on a decoupled scheme

A common approximation often employed to estimate the overall elasto-viscoplastic response (35) consists in homogenizing the elastic and viscoplastic responses in a decoupled fashion (see, for instance, Aravas and Ponte Castañeda, 2004; Segurado et al., 2012). While this approximation is always introduced as *ad hoc*, it actually amounts to bounding from above the incremental effective potential (36) as follows.

Introduce an effective dissipation potential

$$\widetilde{\varphi}(\dot{\overline{\boldsymbol{\alpha}}}) = \min_{\dot{\boldsymbol{\alpha}} \in \mathcal{K}(\dot{\overline{\boldsymbol{\alpha}}})} \left\langle \varphi(\mathbf{x}, \dot{\boldsymbol{\alpha}}) \right\rangle, \tag{41}$$

where $\mathcal{K}(\dot{\bar{\boldsymbol{\alpha}}})$ is the set of traceless compatible (plastic) strain-rate fields with average $\dot{\bar{\boldsymbol{\alpha}}}$. Denote by $\dot{\boldsymbol{\alpha}}^*(\mathbf{x};\, \dot{\bar{\boldsymbol{\alpha}}})$ the minimizer in (41) for a given $\dot{\bar{\boldsymbol{\alpha}}}$. The use of this minimizer as a trial field in (37) then implies the inequality

$$\widetilde{W}_{\Delta}(\dot{\bar{\boldsymbol{\varepsilon}}};\, \boldsymbol{\sigma}_n) \le \widetilde{W}^{\mathrm{dc}}_{\Delta+}(\dot{\bar{\boldsymbol{\varepsilon}}};\, \boldsymbol{\sigma}_n) = \min_{\dot{\bar{\boldsymbol{\alpha}}}} \min_{\dot{\boldsymbol{\varepsilon}}\in\mathcal{K}(\dot{\bar{\boldsymbol{\varepsilon}}})} \left\langle \frac{\Delta t}{2}(\dot{\boldsymbol{\varepsilon}}-\dot{\boldsymbol{\alpha}}^*)\cdot\boldsymbol{\mathcal{L}}(\mathbf{X})(\dot{\boldsymbol{\varepsilon}}-\dot{\boldsymbol{\alpha}}^*) + \boldsymbol{\sigma}_n(\mathbf{X})\cdot(\dot{\boldsymbol{\varepsilon}}-\dot{\boldsymbol{\alpha}}^*) + \varphi(\mathbf{X},\, \dot{\boldsymbol{\alpha}}^*) \right\rangle. \tag{42}$$

Since $\dot{\boldsymbol{\varepsilon}}$ and $\dot{\boldsymbol{\alpha}}^*$ are both compatible, the (elastic) strain rate $\dot{\boldsymbol{\varepsilon}}^e = \dot{\boldsymbol{\varepsilon}} - \dot{\boldsymbol{\alpha}}^*$ is also compatible. Thus, we can write

$$\widetilde{W}^{\mathrm{dc}}_{\Delta+}(\dot{\bar{\boldsymbol{\varepsilon}}};\, \boldsymbol{\sigma}_n) = \min_{\dot{\bar{\boldsymbol{\alpha}}}} \left[\min_{\dot{\boldsymbol{\varepsilon}}^e\in\mathcal{K}(\dot{\bar{\boldsymbol{\varepsilon}}}-\dot{\bar{\boldsymbol{\alpha}}})} \left\langle \frac{\Delta t}{2}\dot{\boldsymbol{\varepsilon}}^e\cdot\boldsymbol{\mathcal{L}}(\mathbf{X})\dot{\boldsymbol{\varepsilon}}^e + \boldsymbol{\sigma}_n(\mathbf{X})\cdot\dot{\boldsymbol{\varepsilon}}^e \right\rangle + \left\langle \varphi(\mathbf{X},\, \dot{\boldsymbol{\alpha}}^*) \right\rangle \right]. \tag{43}$$

Noting that $\langle \boldsymbol{\sigma}_n\cdot\dot{\boldsymbol{\varepsilon}}^e\rangle = \langle\boldsymbol{\sigma}_n\rangle\cdot\langle\dot{\boldsymbol{\varepsilon}}^e\rangle = \bar{\boldsymbol{\sigma}}_n\cdot(\dot{\bar{\boldsymbol{\varepsilon}}}-\dot{\bar{\boldsymbol{\alpha}}})$ by Hill's lemma, and that

$$\min_{\dot{\boldsymbol{\varepsilon}}^e\in\mathcal{K}(\dot{\bar{\boldsymbol{\varepsilon}}}-\dot{\bar{\boldsymbol{\alpha}}})} \left\langle \frac{\Delta t}{2}\dot{\boldsymbol{\varepsilon}}^e\cdot\boldsymbol{\mathcal{L}}(\mathbf{X})\dot{\boldsymbol{\varepsilon}}^e \right\rangle = \frac{\Delta t}{2}(\dot{\bar{\boldsymbol{\varepsilon}}}-\dot{\bar{\boldsymbol{\alpha}}})\cdot\widetilde{\boldsymbol{\mathcal{L}}}(\dot{\bar{\boldsymbol{\varepsilon}}}-\dot{\bar{\boldsymbol{\alpha}}}), \tag{44}$$

where $\widetilde{\boldsymbol{\mathcal{L}}}$ is the effective elastic moduli of the solid, we conclude that

$$\widetilde{W}^{\mathrm{dc}}_{\Delta+}(\dot{\bar{\boldsymbol{\varepsilon}}};\, \boldsymbol{\sigma}_n) = \min_{\dot{\bar{\boldsymbol{\alpha}}}} \left[\frac{\Delta t}{2}(\dot{\bar{\boldsymbol{\varepsilon}}}-\dot{\bar{\boldsymbol{\alpha}}})\cdot\widetilde{\boldsymbol{\mathcal{L}}}(\dot{\bar{\boldsymbol{\varepsilon}}}-\dot{\bar{\boldsymbol{\alpha}}}) + \bar{\boldsymbol{\sigma}}_n\cdot(\dot{\bar{\boldsymbol{\varepsilon}}}-\dot{\bar{\boldsymbol{\alpha}}}) + \widetilde{\varphi}(\dot{\bar{\boldsymbol{\alpha}}}) \right]. \tag{45}$$

Alternatively, the inequality (42) can be obtained by making use of Helmholtz decomposition for $\dot{\boldsymbol{\alpha}}(\mathbf{x})$ in (37) and restricting the divergence-free component to zero. Note that the upper bound (45) depends on the stress field from the previous time step only through the macroscopic average $\bar{\boldsymbol{\sigma}}_n$. The associated overall response

$$\bar{\boldsymbol{\sigma}}_{n+1} = \frac{\partial \widetilde{W}^{\mathrm{dc}}_{\Delta+}}{\partial \dot{\bar{\boldsymbol{\varepsilon}}}}(\dot{\bar{\boldsymbol{\varepsilon}}};\, \bar{\boldsymbol{\sigma}}_n) = \bar{\boldsymbol{\sigma}}_n + \widetilde{\boldsymbol{\mathcal{L}}}(\dot{\bar{\boldsymbol{\varepsilon}}}-\dot{\bar{\boldsymbol{\alpha}}})\Delta t \tag{46}$$

together with the optimality condition in (45) with respect to $\dot{\bar{\boldsymbol{\alpha}}}$ (which is traceless)

$$\mathbf{K}(-\widetilde{\boldsymbol{\mathcal{L}}}(\dot{\bar{\boldsymbol{\varepsilon}}}-\dot{\bar{\boldsymbol{\alpha}}})\Delta t - \bar{\boldsymbol{\sigma}}_n) + \frac{\partial\widetilde{\varphi}}{\partial\dot{\bar{\boldsymbol{\alpha}}}}(\dot{\bar{\boldsymbol{\alpha}}}) = \mathbf{0} \tag{47}$$

imply that

$$\dot{\bar{\boldsymbol{\varepsilon}}} = \widetilde{\boldsymbol{\mathcal{L}}}^{-1}\frac{\bar{\boldsymbol{\sigma}}_{n+1}-\bar{\boldsymbol{\sigma}}_n}{\Delta t} + \frac{\partial\widetilde{\varphi}^\star}{\partial\bar{\boldsymbol{\sigma}}}(\bar{\boldsymbol{\sigma}}_{n+1}), \tag{48}$$

where $\widetilde{\varphi}^\star$ denotes the Legendre dual of $\widetilde{\varphi}$. This is precisely the macroscopic relation assumed by the decoupled scheme: since the effective elasticity tensor is independent of the local dissipation potential and the effective dissipation potential is independent of the local elasticity tensor, the scheme effectively decouples the homogenization problem into a purely elastic problem and a purely viscoplastic problem. In practice, the effective elasticity tensor and dissipation potential cannot be computed exactly so that bounds, such as those of Willis (1981) for $\widetilde{\boldsymbol{\mathcal{L}}}$ and of Ponte Castañeda (1992) for $\widetilde{\varphi}$, must be employed. In any event, the above derivation endows the decoupled scheme with a variational character, at least in the context of infinitesimal deformations. Note that according to this scheme a multiphase solid made up of Maxwellian phases is also Maxwellian, cf. Eq. (32) and (48).

3.4. Estimates based on pointwise-heterogeneous comparison solids

Refined estimates should account for the coupling between the energetic and dissipative processes. Given the non-linearity of the dissipation potential ϕ and the pointwise heterogeneity of the stress field $\boldsymbol{\sigma}_n(\mathbf{x})$, the computation of the coupled, incremental effective potential (37) amounts to solving a *non-linear pointwise*-heterogeneous homogenization problem. With a view to exploiting available results for *linear piecewise*-heterogeneous homogenization problems, we follow Lahellec and Suquet (2013) and introduce the function

$$V_{\Delta}(\eta_0) = \sup_{\dot{\alpha}_{eq}\ge 0} \left\langle \phi(\mathbf{x},\, \dot{\alpha}_{eq}) - \frac{3}{2}\eta_0(\mathbf{x})\dot{\alpha}_{eq}^2 \right\rangle, \tag{49}$$

where η_0 is a linear viscosity field. This definition implies the inequality

$$\langle\phi(\mathbf{x},\, \dot{\alpha}_{eq})\rangle \le \left\langle \frac{3}{2}\eta_0(\mathbf{x})\dot{\alpha}_{eq}^2 \right\rangle + V_{\Delta}(\eta_0) \tag{50}$$

for any combination of scalar fields η_0 and $\dot{\alpha}_{eq}$. This amounts to linearizing the dissipation potential ϕ by means of the secant linearization scheme of Ponte Castañeda (1992) and Suquet (1995). The inequality is useful provided the dissipation potential is sub-quadratic, which is the case of common viscoplasticity models. Eq. (37) and (50) then imply the inequality

$$\widetilde{W}_{\Delta}(\bar{\boldsymbol{\varepsilon}};\boldsymbol{\sigma}_n) \le \inf_{\eta_0\ge 0}\{\widetilde{W}_{\Delta_0}(\bar{\boldsymbol{\varepsilon}};\eta_0)+V_{\Delta}(\eta_0)\}, \tag{51}$$

where the infimum condition yields the best possible bound in terms of the effective potential

$$\widetilde{W}_{\Delta_0}(\bar{\boldsymbol{\varepsilon}};\eta_0) = \min_{\dot{\boldsymbol{\varepsilon}}\in\mathcal{K}(\bar{\boldsymbol{\varepsilon}})}\min_{\dot{\boldsymbol{\alpha}}\in\mathcal{A}}\left\langle \frac{\Delta t}{2}(\dot{\boldsymbol{\varepsilon}}-\dot{\boldsymbol{\alpha}})\cdot\boldsymbol{\mathcal{L}}(\mathbf{X})(\dot{\boldsymbol{\varepsilon}}-\dot{\boldsymbol{\alpha}}) + \boldsymbol{\sigma}_n(\mathbf{X})\cdot(\dot{\boldsymbol{\varepsilon}}-\dot{\boldsymbol{\alpha}}) + \eta_0(\mathbf{X})\dot{\boldsymbol{\alpha}}\cdot\dot{\boldsymbol{\alpha}}\right\rangle \tag{52}$$

of a linearly viscous comparison solid. Carrying out the minimization with respect to $\dot{\boldsymbol{\alpha}}$ in this comparison problem we obtain

$$\widetilde{W}_{\Delta_0}(\bar{\boldsymbol{\varepsilon}};\eta_0) = \min_{\dot{\boldsymbol{\varepsilon}}\in\mathcal{K}(\bar{\boldsymbol{\varepsilon}})}\left\langle \frac{1}{2}\dot{\boldsymbol{\varepsilon}}\cdot\mathbf{L}(\mathbf{X})\dot{\boldsymbol{\varepsilon}} + \boldsymbol{\tau}(\mathbf{X})\cdot\dot{\boldsymbol{\varepsilon}}\right\rangle - \left\langle \frac{1}{4}\frac{1}{\mu(\mathbf{X})\Delta t+\eta_0(\mathbf{X})}\boldsymbol{\sigma}_n^d(\mathbf{X})\cdot\boldsymbol{\sigma}_n^d(\mathbf{X})\right\rangle, \tag{53}$$

where $\mathbf{L}(\mathbf{X}) = 3\kappa_{\Delta}(\mathbf{X})\Delta t\mathbf{J} + 2\mu_{\Delta}(\mathbf{X})\Delta t\mathbf{K}$ is a viscosity tensor,

$$\kappa_{\Delta}(\mathbf{X}) = \kappa(\mathbf{X}), \quad \mu_{\Delta}(\mathbf{X}) = \frac{\eta_0(\mathbf{X})}{\mu(\mathbf{X})\Delta t+\eta_0(\mathbf{X})}\mu(\mathbf{X}), \quad \boldsymbol{\tau}(\mathbf{X}) = \frac{\eta_0(\mathbf{X})}{\mu(\mathbf{X})\Delta t+\eta_0(\mathbf{X})}\boldsymbol{\sigma}_n^d(\mathbf{X}) + \boldsymbol{\sigma}_n^s(\mathbf{X}). \tag{54}$$

Eq. (51) allows the use of available upper bounds or exact results for effective potentials of pointwise-heterogeneous *linear* solids of the form (53) to bound effective potentials of *nonlinear* heterogeneous solids of the form (37). But the minimum problem (53) is precisely the problem considered in Section 2. Thus, by combining the bound (51) with the bound (18) for the comparison problem (53), we can obtain an expression that allows the use of available bounds and exact results for the effective potential of piecewise-heterogeneous linear solids to bound the incremental effective potential of non-linear elasto-viscoplastic solids. For simplicity, however, in this work we make use of the weaker bound (25) rather than the general bound (18). Furthermore, we take the microstructure of the elasto-viscoplastic solid as the microstructure of the comparison solid, that is $\chi_0^{(r)}(\mathbf{x}) = \chi^{(r)}(\mathbf{x})$ for $r = 1, \ldots, N$, and we restrict the class of comparison properties to

$$\eta_0(\mathbf{X}) = \sum_{r=1}^{N}\chi^{(r)}(\mathbf{X})\eta_0^{(r)}, \quad \mathbf{L}_0^{(r)} = 3\kappa_0^{(r)}\Delta t\mathbf{J} + 2\mu_0^{(r)}\Delta t\mathbf{K} \quad \text{and} \quad \mathbf{s}_0(\mathbf{X}) = \boldsymbol{\sigma}_n(\mathbf{X}) - \bar{\boldsymbol{\sigma}}_n. \tag{55}$$

Note that the divergence-free field $\mathbf{s}_0(\mathbf{x})$ is thus identified with the fluctuation of the stress field from the previous time step. The bound for the incremental effective potential (51) then takes the form

$$\widetilde{W}_{\Delta}(\bar{\boldsymbol{\varepsilon}};\boldsymbol{\sigma}_n) \le \widetilde{W}_{\Delta+}(\bar{\boldsymbol{\varepsilon}};\boldsymbol{\sigma}_n) = \inf_{\substack{\boldsymbol{\tau}_0^{(r)},\alpha_0,\\ \eta_0^{(r)},\kappa_0^{(r)},\mu_0^{(r)}}}\left\{\hat{W}_0(\bar{\boldsymbol{\varepsilon}};\kappa_0^{(s)},\mu_0^{(s)},\boldsymbol{\tau}_0^{(s)}) + V(\kappa_0^{(s)},\mu_0^{(s)},\boldsymbol{\tau}_0^{(s)},\eta_0^{(s)},\alpha_0) + \hat{V}_0(\eta_0^{(s)}) + V_{\Delta}(\eta_0^{(s)})\right\}, \tag{56}$$

where the optimization is constrained by the inequalities $\eta_0^{(r)} \ge 0$, $\kappa_0^{(r)} \ge \kappa_{\Delta}^{(r)}$ and $\mu_0^{(r)} \ge \mu_{\Delta}^{(r)}$, the functions $\hat{W}_0$ and V_{Δ} are given by (15) and (49), respectively, and

$$V(\kappa_0^{(s)},\mu_0^{(s)},\boldsymbol{\tau}_0^{(s)},\eta_0^{(s)},\alpha_0) = -\frac{1}{6}\sum_{r=1}^{N}c^{(r)}\frac{1}{(\kappa^{(r)}-\kappa_0^{(r)})\Delta t}\left\langle\Delta\boldsymbol{\tau}^{(r)s}(\mathbf{X})\cdot\Delta\boldsymbol{\tau}^{(r)s}(\mathbf{X})\right\rangle^{(r)} - \frac{1}{4}\sum_{r=1}^{N}c^{(r)}\frac{1}{(\mu_{\Delta}^{(r)}-\mu_0^{(r)})\Delta t}\left\langle\Delta\boldsymbol{\tau}^{(r)d}(\mathbf{X})\cdot\Delta\boldsymbol{\tau}^{(r)d}(\mathbf{X})\right\rangle^{(r)}, \tag{57}$$

$$\hat{V}_0(\eta_0^{(s)}) = -\frac{1}{4}\sum_{r=1}^{N}c^{(r)}\frac{1}{\mu^{(r)}\Delta t+\eta_0^{(r)}}\left\langle\boldsymbol{\sigma}_n^d(\mathbf{X})\cdot\boldsymbol{\sigma}_n^d(\mathbf{X})\right\rangle^{(r)}. \tag{58}$$

It is recalled that the superscripts s and d denote the spherical and deviatoric parts of a tensorial magnitude, respectively, and that

$$\Delta\boldsymbol{\tau}^{(r)}(\mathbf{X}) = \frac{\eta_0^{(r)}}{\mu^{(r)}\Delta t+\eta_0^{(r)}}\boldsymbol{\sigma}_n^d(\mathbf{X}) - \boldsymbol{\tau}_0^{(r)} - \alpha_0[\boldsymbol{\sigma}_n(\mathbf{X})-\bar{\boldsymbol{\sigma}}_n] + \boldsymbol{\sigma}_n^s(\mathbf{X}). \tag{59}$$

When the infimum in (56) corresponds to a stationary point, the various comparison properties are solution to the non-linear system of algebraic equations arising from the stationarity conditions with respect to the comparison properties $\kappa_0^{(r)}$, $\mu_0^{(r)}$, $\boldsymbol{\tau}_0^{(r)}$, α_0 and $\eta_0^{(r)}$.

Differentiation of (56) with respect to the macroscopic strain rate yields an estimate for the overall stress–strain-rate relation; in view of the stationarity conditions, it is given by

$$\bar{\boldsymbol{\sigma}}_{n+1} = \frac{\partial\widetilde{W}_{\Delta+}}{\partial\bar{\boldsymbol{\varepsilon}}}(\bar{\boldsymbol{\varepsilon}};\boldsymbol{\sigma}_n) = \tilde{\mathbf{L}}_0\bar{\boldsymbol{\varepsilon}} + \tilde{\boldsymbol{\tau}}_0, \tag{60}$$

where $\tilde{\mathbf{L}}_0$ and $\tilde{\boldsymbol{\tau}}_0$ are the effective properties of the piecewise heterogeneous solid (15), evaluated at the optimal comparison properties. It is easy to see that in the limiting case of $\{\kappa^{(r)},\mu^{(r)}\}\to\infty$ the various material parameters are such that

$\mu_\Delta^{(r)}\Delta t \to \eta_0^{(r)}$, $\boldsymbol{\tau}(\mathbf{x}) \to \mathbf{0}$, $\hat{V}_0 \to 0$, and $V \to 0$, so that the estimate (56) reduces to that of Ponte Castañeda (1992) and Suquet (1995) for purely viscoplastic solids.

Whether the bound (56) is always sharper than the decoupled bound (45) – assuming the same linearization scheme is employed for the non-linear dissipation potential – is not evident. However, the associated overall response (60) does predict a non-Maxwellian coupling between energetic and dissipative deformation processes in accordance with well-known theorems of homogenization theory (Suquet, 1997). This bound is thus expected to be more accurate than the decoupled bound (48). The comparisons provided in Section 4 for a specific class of material systems are in line with this expectation.

3.4.1. *Simple estimates of the Hashin–Shtrikman type for incompressible power-law solids*

Particularly simple expressions result when the constituent phases are incompressible power-law solids characterized by

$$\kappa^{(r)} \to \infty \quad \text{and} \quad \phi^{(r)}(\dot{\alpha}_{eq}) = \frac{\sigma_0^{(r)}\dot{\varepsilon}_0}{1+m}\left(\frac{\dot{\alpha}_{eq}}{\dot{\varepsilon}_0}\right)^{1+m}, \tag{61}$$

where $\sigma_0^{(r)}$ is a flow stress, $\dot{\varepsilon}_0$ is a reference strain rate, and m is a strain-rate sensitivity exponent such that $0 \le m \le 1$; the limiting values $m=1$ and $m=0$ correspond to linearly viscous and ideally plastic behaviors, respectively.

In this case, $\kappa_0^{(r)} \to \infty$ and the functions V_Δ and V are given by

$$V_\Delta(\eta_0^{(s)}) = \frac{1}{2}\sum_{r=1}^{N} c^{(r)}\frac{1-m}{1+m}\left(\frac{\sigma_0^{(r)}}{\dot{\varepsilon}_0^m}\right)^{2/1-m}\left(\frac{1}{3\eta_0^{(r)}}\right)^{1+m/1-m} \tag{62}$$

and

$$V(\kappa_0^{(s)}, \mu_0^{(s)}, \boldsymbol{\tau}_0^{(s)}, \eta_0^{(s)}, \alpha_0) = -\frac{1}{4}\sum_{r=1}^{N} c^{(r)}\frac{1}{(\mu_\Delta^{(r)} - \mu_0^{(r)})\Delta t}\left\langle \Delta\boldsymbol{\tau}^{d(r)}(\mathbf{x})\cdot\Delta\boldsymbol{\tau}^{d(r)}(\mathbf{x})\right\rangle^{(r)}, \tag{63}$$

where

$$\Delta\boldsymbol{\tau}^{d(r)}(\mathbf{x}) = \left(\frac{\eta_0^{(r)}}{\mu^{(r)}\Delta t + \eta_0^{(r)}} - \alpha_0\right)\boldsymbol{\sigma}_n^d(\mathbf{x}) + \left(\alpha_0\bar{\boldsymbol{\sigma}}_n^d - \boldsymbol{\tau}_0^{(r)}\right). \tag{64}$$

For the special case of statistically isotropic microstructures, suitable bounds of the Hashin–Shtrikman type for piecewise-heterogeneous linear solids are available from the work of Willis (1981). Assuming $\mathbf{L}_0^{(r)} \le \mathbf{L}_0^{(1)}$, the upper bound for $\hat{w}_0$ is given by (15) and (17) with

$$\mathbf{A}^{(r)} = \hat{\mathbf{A}}^{(r)}\left(\sum_{s=1}^{N} c^{(s)}\hat{\mathbf{A}}^{(s)}\right)^{-1}, \quad \mathbf{a}^{(r)} = -\mathbf{P}_0^{(1)}\hat{\mathbf{A}}^{(r)}\left[\boldsymbol{\tau}_0^{(r)} - \sum_{s=1}^{N} c^{(s)}\mathbf{A}^{(s)T}\boldsymbol{\tau}_0^{(s)}\right], \tag{65}$$

$$\hat{\mathbf{A}}^{(r)} = \left[\mathbf{I} + (\mathbf{L}_0^{(r)} - \mathbf{L}_0^{(1)})\mathbf{P}_0^{(1)}\right]^{-1} \quad \text{and} \quad \mathbf{P}_0^{(1)} = (5\mu_\Delta^{(1)}\Delta t)^{-1}\mathbf{K}. \tag{66}$$

If the condition $\mathbf{L}_0^{(r)} \le \mathbf{L}_0^{(1)}$ does not hold, the result ceases to be an upper bound for the effective potential but it can still be used to generate an estimate for the overall stress–strain-rate relation. In fact, Eq. (65) are known to be quite accurate for material systems with particulate microstructures, provided the matrix phase is identified with $r=1$ and the $N-1$ inclusion phases are identified with $r = 2, \ldots, N$.

Now, Eq. (66) imply uniform mechanical fields within the inclusion phases. So, if the initial stress distribution within the elasto-viscoplastic solid is uniform – e.g., nil – then $\boldsymbol{\sigma}_n(\mathbf{x})$ will remain uniform within those phases ($r = 2, \ldots, N$) at every time step. Consequently, the polarization field $(54)_3$ takes the form

$$\tau^d(\mathbf{x}) = \chi^{(1)}(\mathbf{x})\frac{\eta_0^{(1)}}{\mu^{(1)}\Delta t + \eta_0^{(1)}}\boldsymbol{\sigma}_n^d(\mathbf{x}) + \sum_{r=2}^{N}\chi^{(r)}(\mathbf{x})\frac{\eta_0^{(r)}}{\mu^{(r)}\Delta t + \eta_0^{(r)}}\langle\boldsymbol{\sigma}_n^d\rangle^{(r)} = \frac{\eta_0^{(1)}}{\mu^{(1)}\Delta t + \eta_0^{(1)}}[\boldsymbol{\sigma}_n^d(\mathbf{x}) - \bar{\boldsymbol{\sigma}}_n^d]$$

$$+ \frac{\eta_0^{(1)}}{\mu^{(1)}\Delta t + \eta_0^{(1)}}\bar{\boldsymbol{\sigma}}_n^d + \sum_{r=2}^{N}\chi^{(r)}(\mathbf{x})\left(\frac{\eta_0^{(r)}}{\mu^{(r)}\Delta t + \eta_0^{(r)}} - \frac{\eta_0^{(1)}}{\mu^{(1)}\Delta t + \eta_0^{(1)}}\right)\langle\boldsymbol{\sigma}_n^d\rangle^{(r)} \tag{67}$$

in view of the identity $\chi^{(1)}(\mathbf{x}) = 1 - \sum_{r=2}^{N}\chi^{(r)}(\mathbf{x})$. It is now evident that, in this case, the material properties of the comparison solid (53) are within the class (11). Therefore, the optimal comparison parameters will be such that $\mathbf{L}_0^{(r)} = \mathbf{L}^{(r)}$ and $\boldsymbol{\tau}_0(\mathbf{x}) = \boldsymbol{\tau}(\mathbf{x})$, namely

$$\mu_0^{(r)} = \mu_\Delta^{(r)}, \quad \boldsymbol{\tau}_0^{(r)} = \left(\frac{\eta_0^{(r)}}{\mu^{(r)}\Delta t + \eta_0^{(r)}} - \alpha_0 \right) \langle \boldsymbol{\sigma}_n^d \rangle^{(r)} + \alpha_0 \overline{\boldsymbol{\sigma}}_n^d, \quad \text{and} \quad \alpha_0 = \frac{\eta_0^{(1)}}{\mu^{(1)}\Delta t + \eta_0^{(1)}}, \tag{68}$$

so that the effective potential (53) is being uniformized *exactly*. Note that this is possible by virtue of the term $\alpha_0 \mathbf{s}_0(\mathbf{x})$ in the class of comparison polarizations $\boldsymbol{\tau}_0$ admitted. In fact, if the optimal α_0 given by $(68)_3$ is replaced by $\alpha_0 = 0$ and the same values for the other comparison properties are kept, the comparison polarization $\boldsymbol{\tau}_0$ becomes piecewise heterogeneous and the resulting bound reduces to the first-moment approximation of Lahellec and Suquet (2013), which is known to be inaccurate.

Finally, given (68), the bound (56) reduces to

$$\widetilde{W}_{\Delta+}(\dot{\bar{\boldsymbol{\varepsilon}}}; \boldsymbol{\sigma}_n) = \inf_{\eta_0^{(r)} \geq 0} \left\{ \hat{W}_0(\dot{\bar{\boldsymbol{\varepsilon}}}; \eta_0^{(s)}) + \hat{V}_0(\eta_0^{(s)}) + V_\Delta(\eta_0^{(s)}) \right\} \tag{69}$$

and the overall stress–strain-rate relation follows from differentiation according to (60). Finally, the first and second moments of the stress field $\boldsymbol{\sigma}_{n+1}^d(\mathbf{x})$ within each phase r can be estimated by applying the above procedure to the perturbed problem (40) and using the resulting estimate for the incremental effective potential in the identities (38)–(39). The optimality conditions with respect to the viscosities $\eta_0^{(r)}$ in this bound can be written as

$$\frac{1}{3\eta_0^{(r)}\dot{\varepsilon}_0} = \left[\frac{3}{2} \frac{\langle \boldsymbol{\sigma}_c^d \cdot \boldsymbol{\sigma}_c^d \rangle^{(r)}}{(\sigma_0^{(r)})^{2/1-m}} \right]^{1-m/2m} \qquad r = 1, \ldots, N, \tag{70}$$

where $\boldsymbol{\sigma}_c^d(\mathbf{x})$ is the deviatoric stress field associated with the comparison potential $\hat{w}_0$. In the limit of ideal plasticity ($m \to 0$), these conditions reduce to yield conditions of the form

$$\sqrt{\frac{3}{2}\langle \boldsymbol{\sigma}_c^d \cdot \boldsymbol{\sigma}_c^d \rangle^{(r)}} = \sigma_0^{(r)} \quad r = 1, \ldots, N. \tag{71}$$

4. Sample results for particulate composites

4.1. Preliminaries

Sample results are provided here for two-phase composites made up of an elasto-viscoplastic matrix ($r=1$) containing an isotropic dispersion of elastic inclusions ($r=2$). Both phases are taken to be isotropic and incompressible, and the dissipation potential of the matrix material is taken to be of the power-law form (61). The shear moduli are chosen to be $\mu^{(1)} = 10^3\sigma_0^{(1)}$ and $\mu^{(2)} = R\mu^{(1)}$, and the inclusion volume fraction is fixed at $c^{(2)} = 0.3$; the parameter R thus denotes the elastic contrast of the composite.

Specimens are assumed to be initially free of internal stresses and are subjected to deformation histories of the form

$$\bar{\boldsymbol{\varepsilon}}(t) = \bar{\varepsilon}_{ss}(t)(\mathbf{e}_1 \otimes \mathbf{e}_3 + \mathbf{e}_3 \otimes \mathbf{e}_1) + \bar{\varepsilon}_{as}(t)\left(\mathbf{e}_1 \otimes \mathbf{e}_1 - \frac{1}{2}\mathbf{e}_2 \otimes \mathbf{e}_2 - \frac{1}{2}\mathbf{e}_3 \otimes \mathbf{e}_3 \right) \tag{72}$$

relative to an orthonormal basis $\{\mathbf{e}_i\}$, where the first term corresponds to a simple shear along the axis $\mathbf{e}_1$ and the second term corresponds to an axisymmetric shear about that axis. Three different loading programs are studied:

LOADING 1. Radial deformation consisting of a triangular axisymmetric shear:

$$\bar{\varepsilon}_{ss}(t) = 0 \quad \text{and} \quad \bar{\varepsilon}_{as}(t) = \frac{\dot{\gamma}}{T_0}\left(t - 2T_0 \left\lfloor \frac{t}{2T_0} + \frac{1}{2} \right\rfloor \right)(-1)^{\left\lfloor \frac{t}{2T_0} + \frac{1}{2} \right\rfloor}, \tag{73}$$

where $\lfloor \cdot \rfloor$ denotes the floor function.

LOADING 2. Radial deformation consisting of an axisymmetric loading ramp up to a constant value:

$$\bar{\varepsilon}_{ss}(t) = 0 \quad \text{and} \quad \bar{\varepsilon}_{as}(t) = \begin{cases} \dot{\gamma}t & 0 \leq t \leq T_0 \\ \dot{\gamma}T_0 & T_0 < t \end{cases}. \tag{74}$$

LOADING 3. Rotating deformation:

$$\bar{\varepsilon}_{ss}(t) = \frac{\sqrt{3}}{4}\gamma[1 - \cos(\omega t)] \quad \text{and} \quad \bar{\varepsilon}_{as}(t) = \gamma \sin(\omega t). \tag{75}$$

The constants γ, $\dot{\gamma}$, T_0, and ω are loading parameters specified below.

The new estimates are compared with the earlier estimates of Lahellec and Suquet (2003, 2007a,2013). These earlier estimates are all based on piecewise-heterogeneous comparison solids and hinge upon different uniformization schemes.

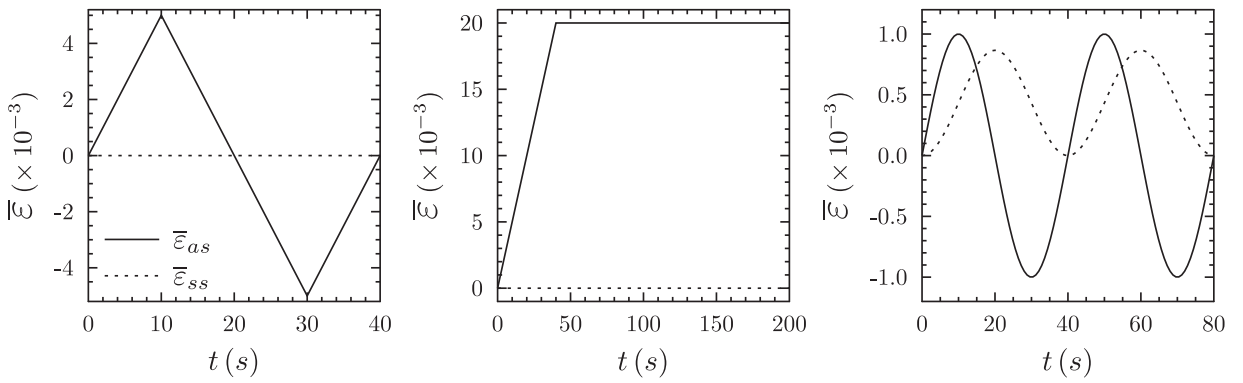

Fig. 1. Loading programs considered: (a) Radial deformation consisting of a triangular axisymmetric shear (program 1), (b) radial deformation consisting of an axisymmetric loading ramp up to a constant value (program 2), (c) rotating deformation (program 3). The functions $\varepsilon_{as}(t)$ (continuous lines) and $\varepsilon_{ss}(t)$ (dotted lines) yield the time-dependent axisymmetric and simple shear components, respectively.

The estimates of Lahellec and Suquet (2003, 2007a) make use of an incremental variational principle with strains as primal variables – rather than strain rates as in (36) – and uniformize the plastic strain field at the current time step; we refer to them as "effective internal variable" estimates. The more recent estimates of Lahellec and Suquet (2013) make use of the incremental variational principle (36) with strain rates as primal variables, but uniformize the stress field from the previous time step; we refer to them as "effective stress" estimates. The new estimates, by contrast, uniformize the polarization field at the current time step; we refer to them as "effective polarization" estimates. In all cases, the same secant linearization and linear Hashin–Shtrikman estimates are employed. Thus, the new estimates are computed by means of the expressions provided in Section 3.4.1, which require the numerical solution of one non-linear equation for the optimal comparison viscosity $\eta_0^{(1)}$ in the matrix phase, as given by Eq. (70) with $r=1$.

The accuracy of the predictions is assessed by confronting them to full-field simulations of periodic composites with unit cells containing a monodisperse distribution of fifty spherical inclusions randomly placed at the prescribed volume fraction, see Fig. 2a. The field equations are solved by means of a computational method based on the Fast Fourier Transform originally proposed by Moulinec and Suquet (1998) and implemented in the software CRAFT (available at http://craft.lma.cnrs-mrs.fr). The results provided below make use of a regular array of 256^3 Fourier points. To obtain representative results for material systems exhibiting statistical homogeneity and overall isotropy, the macroscopic responses of ten different realizations were evaluated. Fig. 2b shows the maximum, minimum and average stress levels obtained for a rate-independent elasto-plastic composite with compliant inclusions ($m=0$, $R=0.2$) subject to the loading program 1 of Fig. 1a. Given the negligible dispersion observed, only the softer realization is considered henceforth.

4.2. Results and discussion

Fig. 3 shows predictions for rate-independent elasto-plastic specimens ($m=0$) subjected to the radial loading program 1 of Fig. 1a with $\dot{\gamma} = 5{\cdot}10^{-4}\ s^{-1}$ and $T_0 = 10$ s, see parts (a)–(c), and to rotating loading program 3 of Fig. 1c with $\gamma = 10^{-3}$ and $\omega = \pi/20$ rad/s, see parts (d)–(e). Three values of elastic contrast R corresponding to compliant ($R=0.2$), uniform ($R=1$) and stiff

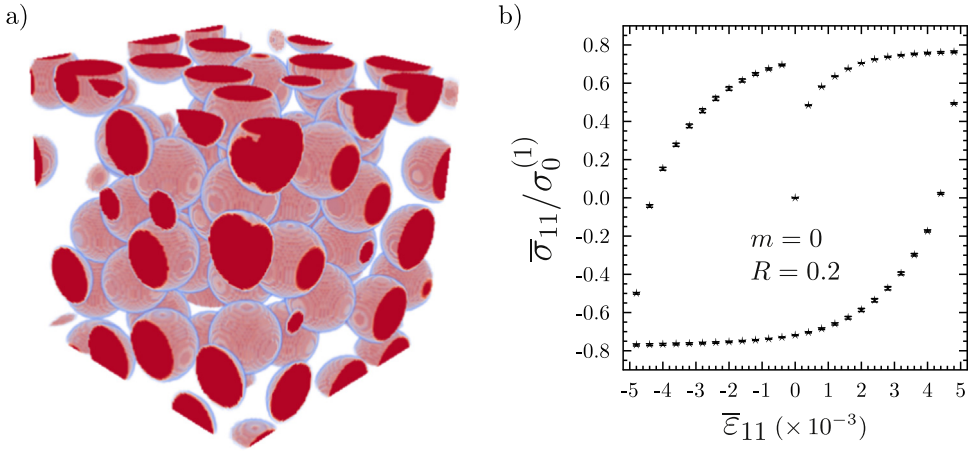

Fig. 2. Full-field simulations: (a) A unit cell realization containing a monodisperse distribution of fifty spherical inclusions at a volume fraction $c^{(2)} = 0.3$; (b) overall responses of ten realizations with $m=0$, $\mu^{(1)} = 10^3\sigma_0^{(1)}$ and $\mu^{(2)} = 0.2\mu^{(1)}$, subject to loading program 1 of Fig. 1a.

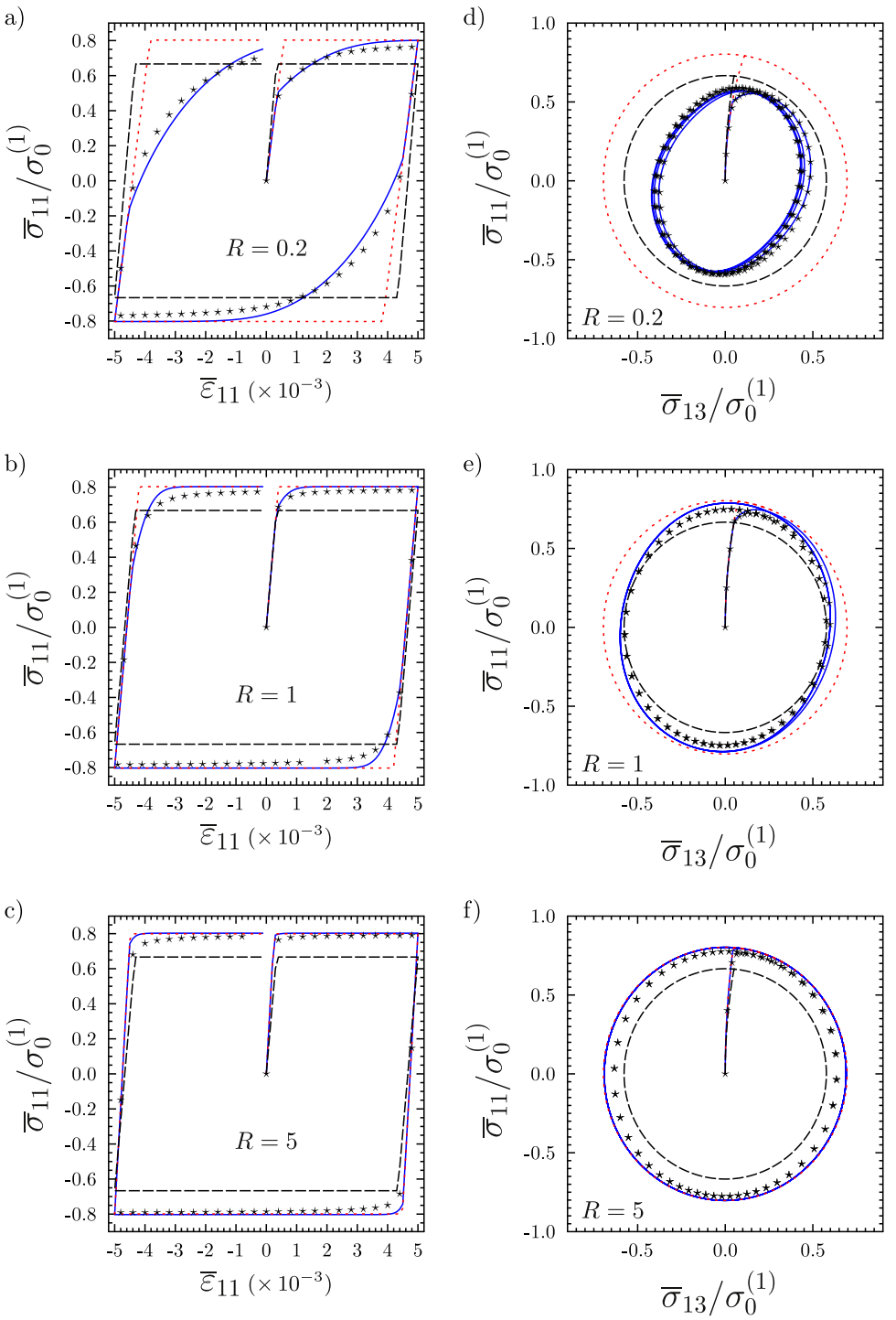

Fig. 3. Results for elasto-plastic solids ($m=0$) with three elastic contrasts (R = 0.2, 1, 5), subjected to the loading programs 1 (left) and 3 (right) of Fig. 1a,c. The new estimates (continuous lines) are compared with estimates based on the decoupled scheme (dotted lines), FFT full-field simulations (symbols), and the monolithic matrix response (dashed lines). The volume fraction of inclusions is $c^{(2)} = 0.3$.

($R=5$) inclusions are considered. The new "effective polarization" estimates (continuous lines) are compared with estimates based on the decoupled scheme (dotted lines) and FFT full-field simulations (symbols). The time step employed in the computations of all estimates is $\Delta t = 10^{-3}$ s. The response of the monolithic matrix material (dashed lines) is also included for reference.

We begin by noting that in the absence of second-phase inclusions the (matrix) response under loading program 1 is elastic-perfectly plastic with tension-compression symmetry and no elastic–plastic transition nor plastic hardening, and

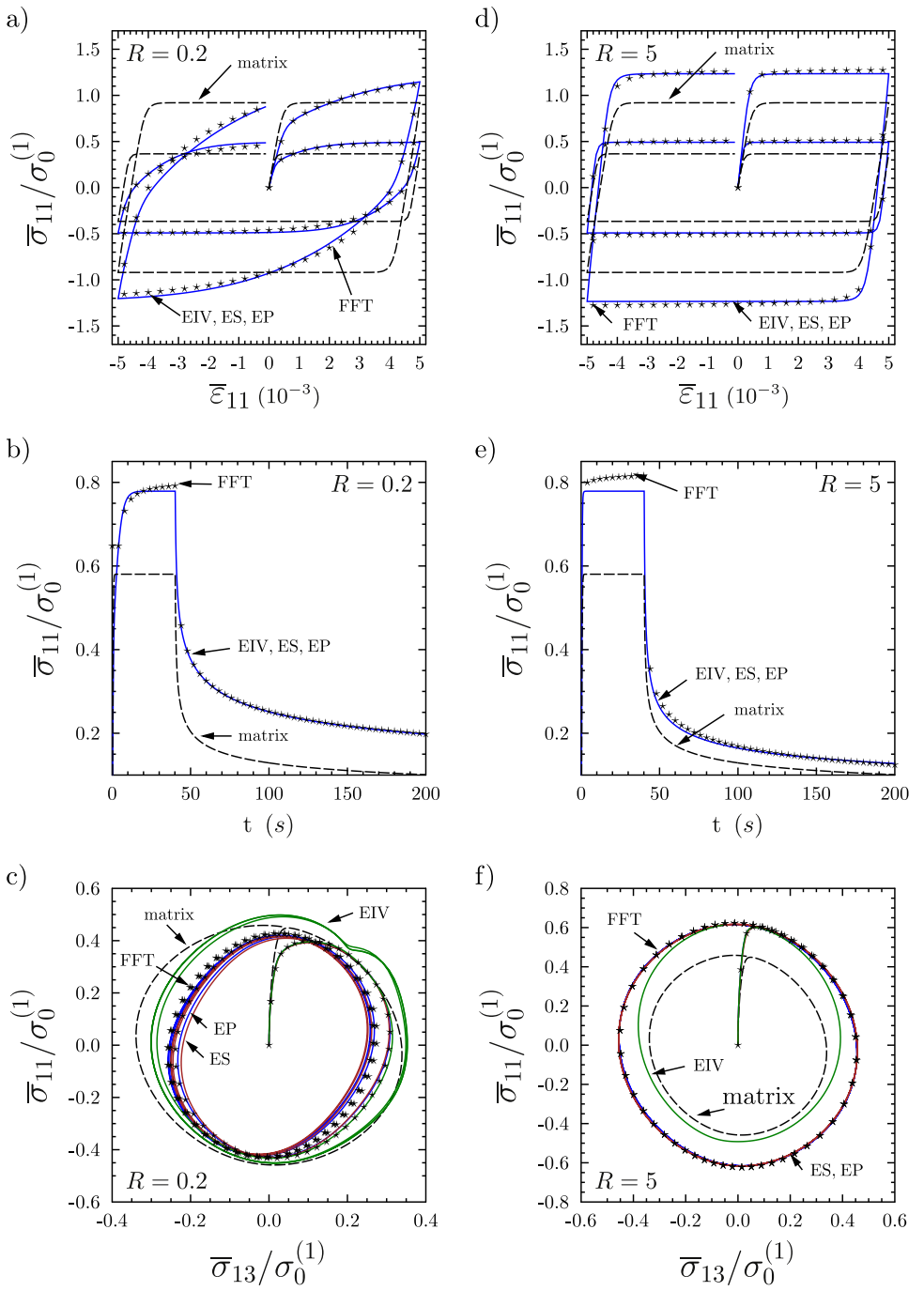

Fig. 4. Results for elasto-viscoplastic solids (m=0.2) with two elastic contrasts (R = 0.2, 5), subjected to loading programs 1 (with two different strain rates), 2 and 3. The new estimates (continuous lines blue) are compared with EIV estimates (continuous lines green), ES estimates (continuous lines brown), FFT full-field simulations (symbols) and the monolithic matrix response (dashed lines). The volume fraction of inclusions is $c^{(2)}$ = 0.3. (For interpretation of the references to color in this figure caption, the reader is referred to the web version of this paper.)

under loading program 3 stabilizes on a circular path in stress space. By contrast, the FFT results show that in the presence of second-phase inclusions the response under loading program 1 can exhibit significant tension-compression asymmetry (Bauschinger effect) and wide elasto-plastic transitions, see parts (a)–(c), and under loading program 3 can describe non-circular stress paths, see parts (d)–(f). These macroscopic constitutive features induced by microscopic material heterogeneity are pronounced in the case of compliant inclusions but subtle in the case of stiff inclusions. In fact, the case of compliant inclusions is somewhat peculiar for it corresponds to inclusions exhibiting a low elastic modulus but an infinite plastic strength. Such a combination of material properties induces a wide elasto-plastic transition in the macroscopic

response, for the initial elastic limit must be lower than that of the matrix material but the plastic limit must be higher, see part (a). In any event, regardless of its relevance to real material systems, this peculiarity makes it a particularly stringent test case for approximate estimates like the ones proposed in this work.

The new estimates are found to be in good agreement with the FFT results for all cases considered. Thus, these estimates are able to capture elasto-plastic transitions, tension-compression asymmetries, and stress-path distortions induced by material heterogeneity. Furthermore, under loading program 1, they correctly asymptote deep in the plastic range to the stress level predicted by the corresponding rigid-plastic estimates, as shown in Appendix B. By contrast, estimates based on the popular decoupled scheme are seen to be accurate in the case of stiff inclusions, see parts (c) and (f), but to deteriorate significantly in the case of compliant inclusions. This is because the decoupled scheme predicts a macroscopic Maxwellian response and is therefore completely unable to capture elasto-plastic transitions, tension-compression asymmetries and stress-path distortions regardless of microscopic material heterogeneity.

Fig. 4 shows predictions for elasto-viscoplastic solids with strain-rate sensitivity $m=0.2$, subjected to radial loading program 1 with various strain rates ($\dot{\gamma} = 5{\cdot}10^{-5}\,\mathrm{s}^{-1},\ 5{\cdot}10^{-3}\,\mathrm{s}^{-1}$) and $T_0 = 10$ s, see parts (a)–(b), to rotating loading program 3 with $\gamma = 10^{-3}$ and $\omega = \pi/20$ rad/s, see parts (d)–(e), and to radial program 2 with $\dot{\gamma} = 5{\cdot}10^{-4}\,\mathrm{s}^{-1}$ and $T_0 = 40$ s. Two values of elastic contrast R corresponding to compliant ($R=0.2$) and stiff ($R=5$) inclusions are considered. The new estimates are compared with the "effective internal variable" (EIV) estimates of Lahellec and Suquet (2007b) and "effective stress" (ES) estimates of Lahellec and Suquet (2013), and with FFT full-field simulations. Once again, the response of the monolithic matrix material (dashed lines) is also included for reference.

We begin by noting that all estimates give virtually the same predictions – within numerical accuracy – for radial loading programs 1 and 3, and that these predictions are in good agreement with the FFT results for both elastic contrasts. Thus, all estimates correctly capture the effect of material heterogeneity on the rate-dependent elasto-plastic transition, tension-compression asymmetry and stress relaxation of the composite solid. Differences are found, however, between the predictions for rotating loading program 2. For this loading condition, the EIV estimates are seen to be quite off the FFT results and, more strikingly, predict a lobular stress path for the case of compliant inclusions which is at odds with the FFT results, see part (b). The EP and ES estimates, on the other hand, remain in good agreement with the FFT results. The improvement of these last two estimates over the earlier EIV estimates is therefore attributed to the use of incremental variational principles based on strain rates rather than strains, and not to the use of a pointwise-heterogeneous comparison solid. However, the use of pointwise-heterogeneous comparison solids in the EP estimates does prove convenient in view of the fact that the EP and ES estimates exhibit similar accuracy but the EP estimates involve a single non-linear equation while the ES estimates involve two. In other words, the use of pointwise-heterogeneous comparison solids can lead to simplified optimality conditions without loss of accuracy. In this connection, Badulescu et al. (2015) have recently applied the "effective stress" estimates of Lahellec and Suquet (2013) to a model class of linear viscoelastic polycrystals. Acceptable predictions were obtained for monotonic loadings but technical issues related to optimality conditions with multiple roots were identified for cyclic loadings. The above observations suggest that the use of more general pointwise-heterogeneous comparison solids in the context of polycrystalline systems may simplify the optimality conditions and consequently remedy the alluded technical issues. Efforts to clarify this point are currently under way and will be reported upon completion.

Acknowledgements

The authors are grateful to Prof. P. Suquet for helpful discussions; this contribution is dedicated to him with deep admiration and affection. The work was funded by a CONICET-CNRS international collaboration through grants PCB-II D5054 and PICS 06400. M.I.I. acknowledges additional support from UNLP through grant I-2013-179.

Appendix A. Effective potential of pointwise-heterogeneous comparison solid

Let

$$\boldsymbol{\tau}_0^p(\mathbf{x}) = \sum_{r=1}^{N} \chi_0^{(r)}(\mathbf{x})\boldsymbol{\tau}_0^{(r)}, \tag{76}$$

and note that the constraints (12)–(13) imply that

$$\langle \alpha_0 \mathbf{s}_0 {\cdot} \dot{\boldsymbol{\varepsilon}} \rangle = \alpha_0 \langle \mathbf{s}_0 \rangle {\cdot} \langle \dot{\boldsymbol{\varepsilon}} \rangle = 0 \quad \text{and} \quad \dot{\boldsymbol{\varepsilon}} - \beta_0 \boldsymbol{\gamma}_0 \in \mathcal{K}(\tilde{\boldsymbol{\varepsilon}}) \quad \text{for any } \dot{\boldsymbol{\varepsilon}} \in \mathcal{K}(\tilde{\boldsymbol{\varepsilon}}). \tag{77}$$

Then,

$$\widetilde{w}_0(\bar{\dot{\boldsymbol{\varepsilon}}};\mathbf{L}_0,\boldsymbol{\tau}_0)=\min_{\dot{\boldsymbol{\varepsilon}}\in\mathcal{K}(\bar{\dot{\boldsymbol{\varepsilon}}})}\langle w_0(\mathbf{x},\dot{\boldsymbol{\varepsilon}})\rangle=\min_{\dot{\boldsymbol{\varepsilon}}\in\mathcal{K}(\bar{\dot{\boldsymbol{\varepsilon}}})}\left\langle\frac{1}{2}\dot{\boldsymbol{\varepsilon}}\cdot\mathbf{L}_0(\mathbf{x})\dot{\boldsymbol{\varepsilon}}+\boldsymbol{\tau}_0(\mathbf{x})\cdot\dot{\boldsymbol{\varepsilon}}\right\rangle=\min_{\dot{\boldsymbol{\varepsilon}}\in\mathcal{K}(\bar{\dot{\boldsymbol{\varepsilon}}})}\left\langle\frac{1}{2}\dot{\boldsymbol{\varepsilon}}\cdot\mathbf{L}_0(\mathbf{x})\dot{\boldsymbol{\varepsilon}}+[\boldsymbol{\tau}_0^p(\mathbf{x})+\alpha_0\mathbf{s}_0(\mathbf{x})+\beta_0\mathbf{L}_0(\mathbf{x})\boldsymbol{\gamma}_0(\mathbf{x})]\cdot\dot{\boldsymbol{\varepsilon}}\right\rangle$$
$$=\min_{\dot{\boldsymbol{\varepsilon}}\in\mathcal{K}(\bar{\dot{\boldsymbol{\varepsilon}}})}\left\langle\frac{1}{2}\dot{\boldsymbol{\varepsilon}}\cdot\mathbf{L}_0(\mathbf{x})\dot{\boldsymbol{\varepsilon}}+[\boldsymbol{\tau}_0^p(\mathbf{x})+\beta_0\mathbf{L}_0(\mathbf{x})\boldsymbol{\gamma}_0(\mathbf{x})]\cdot\dot{\boldsymbol{\varepsilon}}\right\rangle=\min_{\dot{\boldsymbol{\varepsilon}}\in\mathcal{K}(\bar{\dot{\boldsymbol{\varepsilon}}})}\left\langle\frac{1}{2}(\dot{\boldsymbol{\varepsilon}}-\beta_0\boldsymbol{\gamma}_0)\cdot\mathbf{L}_0(\mathbf{x})(\dot{\boldsymbol{\varepsilon}}-\beta_0\boldsymbol{\gamma}_0)\right.$$
$$\left.+[\boldsymbol{\tau}_0^p(\mathbf{x})+\beta_0\mathbf{L}_0(\mathbf{x})\boldsymbol{\gamma}_0(\mathbf{x})]\cdot(\dot{\boldsymbol{\varepsilon}}-\beta_0\boldsymbol{\gamma}_0)\right\rangle=\min_{\dot{\boldsymbol{\varepsilon}}\in\mathcal{K}(\bar{\dot{\boldsymbol{\varepsilon}}})}\left\langle\frac{1}{2}\dot{\boldsymbol{\varepsilon}}\cdot\mathbf{L}_0(\mathbf{x})\dot{\boldsymbol{\varepsilon}}+\boldsymbol{\tau}_0^p(\mathbf{x})\cdot\dot{\boldsymbol{\varepsilon}}\right\rangle$$
$$+\left\langle\frac{1}{2}\beta_0^2\boldsymbol{\gamma}_0(\mathbf{x})\cdot\mathbf{L}_0(\mathbf{x})\boldsymbol{\gamma}_0(\mathbf{x})-\beta_0\boldsymbol{\tau}_0^p(\mathbf{x})\cdot\boldsymbol{\gamma}_0(\mathbf{x})\right\rangle=\hat{w}_0(\bar{\dot{\boldsymbol{\varepsilon}}};\mathbf{L}_0^{(s)},\boldsymbol{\tau}_0^{(s)})+\hat{v}_0(\mathbf{L}_0^{(s)},\boldsymbol{\tau}_0^{(s)},\beta_0),$$

where the potential $\hat{w}_0$ is given by (15) and the function $\hat{v}_0$ is given by (16).

Appendix B. Asymptotic behavior of new estimates deep in the plastic range

At time step $n+1$, the macroscopic stress $\bar{\boldsymbol{\sigma}}_{n+1}^d=\langle\boldsymbol{\sigma}_{n+1}\rangle$ and stress statistics $\langle\boldsymbol{\sigma}_{n+1}^d\rangle^{(r)}$ and $\langle\boldsymbol{\sigma}_{n+1}^d\cdot\boldsymbol{\sigma}_{n+1}^d\rangle^{(r)}$ predicted by the new estimates of the Hashin–Shtrikman type for elasto-viscoplastic solids derived in Section 3.4.1 are equal to the corresponding volume averages of the stress field $\boldsymbol{\sigma}_c$ associated with the linear-comparison solid in (69). This follows from the facts that the estimate (69) is stationary with respect to the $\eta_0^{(r)}$'s and that the Hashin–Shtrikman estimate for the linear-comparison solid is realizable. The stress field $\boldsymbol{\sigma}_c$ solves the equations

$$\nabla\cdot\boldsymbol{\sigma}_c(\mathbf{x})=\mathbf{0},\tag{78}$$

$$\boldsymbol{\sigma}_c(\mathbf{x})=2\mu_0(\mathbf{x})\Delta t\;\dot{\boldsymbol{\varepsilon}}_c(\mathbf{x})+\boldsymbol{\tau}_0(\mathbf{x})-p(\mathbf{x})\mathbf{I},\tag{79}$$

$$\dot{\boldsymbol{\varepsilon}}_c(\mathbf{x})=\nabla\otimes_s\;\dot{\mathbf{u}}_c,\quad \operatorname{tr}\dot{\boldsymbol{\varepsilon}}_c(\mathbf{x})=0,\quad \langle\dot{\boldsymbol{\varepsilon}}_c(\mathbf{x})\rangle=\bar{\dot{\boldsymbol{\varepsilon}}},\tag{80}$$

defined over the representative volume element. In view of (54) and (68), the deviatoric part of the constitutive law (79) is given by

$$\boldsymbol{\sigma}_c^d(\mathbf{x})=2\mu(\mathbf{x})\Delta t\frac{\eta_0(\mathbf{x})}{\mu(\mathbf{x})\Delta t+\eta_0(\mathbf{x})}\dot{\boldsymbol{\varepsilon}}_c(\mathbf{x})+\frac{\eta_0(\mathbf{x})}{\mu(\mathbf{x})\Delta t+\eta_0(\mathbf{x})}\boldsymbol{\sigma}_n^d(\mathbf{x}).\tag{81}$$

Deep in the plastic range the stress reaches a steady state. Thus, $\boldsymbol{\sigma}_c^d(\mathbf{x})=\boldsymbol{\sigma}_n^d(\mathbf{x})$ and in view of (81)

$$\boldsymbol{\sigma}_c^d(\mathbf{x})=2\eta_0(\mathbf{x})\dot{\boldsymbol{\varepsilon}}_c(\mathbf{x}),\tag{82}$$

where η_0 is the optimal viscosity that solves Eqs. (70). The quantities η_0 and $\bar{\boldsymbol{\sigma}}_{n+1}^d$ thus reduce exactly to those of Ponte Castañeda (1992) and Suquet (1995) for purely viscoplastic solids.

References

Aravas, N., Ponte Castañeda, P., 2004. Numerical methods for porous metals with deformation-induced anisotropy. Comput. Methods Appl. Mech. Eng. 193, 3767–3805.

Badulescu, C., Lahellec, N., Suquet, P., 2015. Field statistics in linear viscoelastic composites and polycrystals. Eur. J. Mech. Solids 49, 329–344.

Germain, P., Nguyen, Q., Suquet, P., 1983. Continuum thermodynamics. J. Appl. Mech. 50, 1010–1020.

Hill, R., 1965. Continuum micro-mechanics of elastoplastic polycrystals. J. Mech. Phys. Solids 13, 89–101.

Idiart, M.I., 2014. Modeling two-phase ferroelectric composites by sequential laminates. Model. Simul. Mater. Sci. Eng. 22, 025010.

Idiart, M.I., Ponte Castañeda, P., 2007. Field statistics in nonlinear composites I. Theory Proc. R. Soc. A 463, 183–202.

Lahellec, N., Suquet, P., 2003. Composites non linéaires à deux potentiels: estimations affine et du second-order. In: Potier-Ferry, M., Bonnet, M., Bignonnet, A. (Eds.), 6ème Colloque National en Calcul des Structures. Tome 3. CSMA, pp. 49–56.

Lahellec, N., Suquet, P., 2007a. Effective behavior of linear viscoelastic composites: a time-integration approach. Int. J. Solids Struct. 44, 507–529.

Lahellec, N., Suquet, P., 2007b. On the effective behavior of nonlinear inelastic composites: I. Incremental variational principles. J. Mech. Phys. Solids 55, 1932–1963.

Lahellec, N., Suquet, P., 2013. Effective response and field statistics in elasto-plastic and elasto-viscoplastic composites under radial and non-radial loadings. Int. J. Plast. 42, 1–30.

Lahellec, N., Ponte Castañeda, P., Suquet, P., 2011. Variational estimates for the effective response and field statistics in thermoelastic composites with intra-phase property fluctuations. Proc. R. Soc. A 467, 2224–2246.

Masson, R., Bornert, M., Suquet, P., Zaoui, A., 2000. An affine formulation for the prediction of the effective properties of nonlinear composites and polycrystals. J. Mech. Phys. Solids 48, 1203–1227.

Miehe, C., 2002. Strain-driven homogenization of inelastic microstructures and composites based on an incremental variational formulation. Int. J. Numer. Methods Eng. 55, 1285–1322.

Miehe, C., Rosato, D., 2011. A rate-dependent incremental variational formulation of ferroelectricity. Int. J. Eng. Sci. 49, 466–496.

Moulinec, H., Suquet, P., 1998. A numerical method for computing the overall response of nonlinear composites with complex microstructure. Comp. Methods Appl. Mech. Eng. 157, 69–94.

Ponte Castañeda, 1992. New variational principles in plasticity and their application to composite materials. J. Mech. Phys. Solids 40, 1757–1788.

Ponte Castañeda, P., Suquet, P., 1998. Nonlinear composites. Adv. Appl. Mech. 34, 171–302.

Segurado, J., Lebensohn, R.A., LLorca, J., Tomé, C.N., 2012. Multiscale modeling of plasticity based on embedding the viscoplastic self-consistent formulation in implicit finite elements. Int. J. Plast. 28, 124–140.
Suquet, P., 1995. Overall properties of nonlinear composites: a modified secant moduli theory and its link with Ponte Castañeda's nonlinear variational procedure. C.R. Acad. Sci. Paris, Série IIb 320, 563–571.
Suquet, P., 1997. Effective properties of nonlinear composites. In: Suquet, P. (Ed.), Continuum Micromechanics. CISM Lecture Notes, vol. 377. . Springer-Verlag, New York, pp. 197–264.
Willis, J.R., 1981. Variational and Related Methods for the Overall Properties of Composites. Adv. Appl. Mech. 21, 1–78.
Withers, P.J., 2007. Residual stress and its role in failure. Rep. Progr. Phys. 70, 2211–2264.